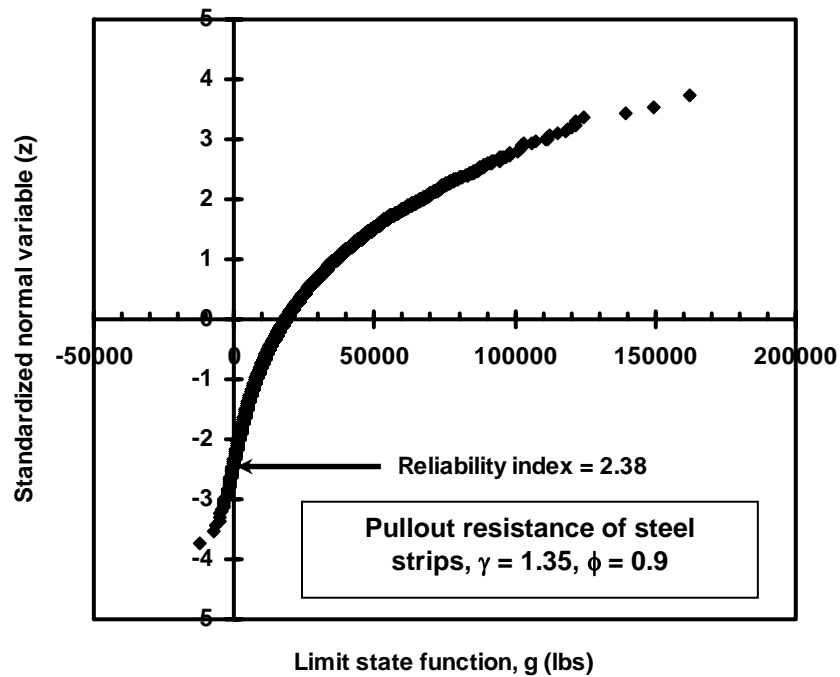


REPORT

LRFD CALIBRATION OF COHERENT GRAVITY METHOD FOR METALLICALLY REINFORCED MSE WALLS



BY:
D'APPOLONIA ENGINEERING

PREPARED FOR:
ASSOCIATION FOR METALLICALLY STABILIZED EARTH

DECEMBER 2007



Executive Summary

Beginning with the Interims to the 1991 AASHTO Standard Specifications for Highway Bridges (*Standard Specifications*), the *Standard Specifications* permitted the maximum load at each reinforcement level to be computed using the:

- Coherent Gravity Method;
- Tieback Wedge Method; or
- Structure Stiffness Method

In the late 1990s, Technical Committee T-15 on Substructures and Retaining Walls of the AASHTO Subcommittee on Bridges and Structures developed the Simplified Method which was included in the 1999 interims to the *Standard Specifications* and the *LRFD Specifications*.

Article 11.10.6.2.1 of the *LRFD Specifications* (2007) requires that the maximum load in reinforcements be calculated using the Simplified Method approach along with the prescribed resistance factors calibrated for the method. So while the LRFD Specifications allows “other widely accepted and published design methods” to be used “for calculation of reinforcement loads”, alternative methods (e.g., Coherent Gravity) are permitted only “if the wall designer develops method-specific resistance factors for the method employed”. Therefore, the objective of the study is to develop resistance factors for the internal stability design of metallicity reinforced MSE walls using the Coherent Gravity Method.

D’Appolonia compiled a worldwide database of selected, well documented MSEW case studies from the literature and through personal communications. The database includes 17 full-scale metallicity reinforced MSE walls (22 wall sections). The walls were constructed between 1972 and 1998 and the wall sections represent typical RECO and York (steel strips), VSL (bar mats) and Hilfiker (welded wires) type walls. The wall sections were instrumented to evaluate their field performance and measure in-situ stresses and deformations of steel reinforcements due to static earth loads during and for short-term periods after construction. For this study, our primary interest focused is on deformations and tensile stresses measured on the steel reinforcements. Other field measurements such as soil vertical and horizontal pressures are used to generally check the validity of soil backfill properties used in the design.

Calibration of the Coherent Gravity Method is conducted using Monte Carlo simulation, which is the approach preferred by AASHTO for calibrating load and resistance factors for the *LRFD Specifications*. The Monte Carlo method is simply a technique that utilizes a random number generator to extrapolate the limit state functions, g , for calibration of the pullout and rupture resistances. In the Monte Carlo analyses, random values of g were generated using the mean, standard deviation, and the distribution type (normal or lognormal) of the bias of the load (i.e., maximum tension in steel reinforcement) and the resistance (i.e., pullout or rupture). The loads were calculated using the lateral earth pressure coefficient in the *Standard Specifications* (AASHTO, 1996), which is compatible with the Coherent Gravity Method of design for checking internal stability of MSE reinforcements. A calibration was performed twice for each design mode. One calibration was performed ignoring the steel corrosion (i.e., end of construction case) when the field monitoring data were collected. The second calibration was performed considering steel corrosion through 75 years (assumed structure design life) using the AASHTO corrosion model for metallic reinforcements (AASHTO, 1996 and 2007). The extrapolation of g makes estimating β possible when γ and ϕ are assumed. A value of $\gamma = 1.35$ was adopted compatible with the static earth load conditions (AASHTO, 2007). A range of ϕ values was



assumed and estimated values of β (by iteration) were checked against a typical range of β (3.5 to 2.3) used in previous LRFD calibrations.

The Monte Carlo calibration analyses resulted in β values consistent with the range for the pullout resistance of steel strips and steel grids from previous LRFD calibrations. The analysis indicated that for $\phi = 0.9$, reasonable β values of 2.33 and 2.60 were computed for pullout resistance of steel strips and steel grids, respectively. The reasonableness of the β values was checked against values determined using closed-form solutions. Based on the results of these analyses, D'Appolonia recommends $\phi = 0.9$ for the pullout resistance of steel strips and steel grids using the Coherent Gravity Method which is the same value prescribed in the *LRFD Specifications* (AASHTO, 2007) for pullout resistance using the Simplified Method.

The calibration analyses of the steel rupture resistance resulted in β values > 3.50 , which is greater than typical values of β determined in previous LRFD calibrations. Similar results were obtained using calibration closed-form solutions. The high values of β are attributed to the much higher additional resistance provided by the steel reinforcements at rupture compared to the loads measured in the instrumented test sections which represent service loading. The *LRFD Specifications* (AASHTO, 2007) specify $\phi = 0.75$ for steel strips and $\phi = 0.65$ for steel grids for the Simplified Method, which correspond to $0.55F_y$ for steel strips and $0.48F_y$ ^[1] for steel grids in allowable stress design (ASD). D'Appolonia believes that the currently used ϕ values are overly conservative, and recommends $\phi = 0.90$ for the rupture resistance of steel strips and $\phi = 0.80$ for the rupture resistance of steel grids using the Coherent Gravity Method.

[1] The lower value of F_y for steel grids takes into account the potential for interior wires to be more highly stressed than exterior wires of a grid reinforcement element.



Table of Contents

Executive Summary	i
1. Introduction.....	1
2. Database.....	2
2.1 Database Statistics.....	3
3. Load-Resistance Calculation.....	3
4. Calibration Using Monte Carlo Analysis	9
4.1 A Monte Carlo Simulation Example	14
4.2 Monte Carlo Simulation Analyses.....	16
4.3 Calibration of Pullout Resistance	16
4.3.1 Calibration of Pullout Resistance for Steel Strips	16
4.3.2 Calibration of Pullout Resistance for Steel Grids.....	18
4.4 Calibration of Rupture Resistance.....	20
4.4.1 Calibration of Rupture Resistance for Steel Strips	20
4.4.2 Calibration of Rupture Resistance for Steel Grids.....	21
4.5 Verification of Monte Carlo Analysis Results.....	22
5. Recommendations	23
Acknowledgments.....	23
References	24
Appendix A: Summary of Wall Geometries, Backfill Properties and Steel Reinforcement Details	A-1
Appendix B: Calibration Results of Steel Pullout Resistance and Steel Rupture Resistance Using Monte Carlo Analysis.....	B-1



LIST OF ABBREVIATIONS

AASHTO	= American Association of State Highway and Transportation Officials
AMSE	= Association for Metallically Stabilized Earth
ASD	= allowable stress design
CDF	= cumulative distribution function
LRFD	= load and resistance factor design
MSE	= mechanically stabilized earth

LIST OF SYMBOLS

A	= tributary area of a steel strip or grid (sf)
A_c	= steel area corrected for corrosion (in ²)
b	= width of reinforcement (in)
C	= effective unit perimeter of reinforcement = 2 (dim)
COV	= coefficient of variation (dim)
C_u	= uniformity coefficient of backfill (dim)
F^*	= pullout resistance factor, which is a function of passive and frictional resistance of reinforcement (see Table 5) (dim)
F_y	= steel yield strength (ksi)
g	= random variable representing the safety margin
H	= wall height (ft)
K	= coefficient of lateral earth pressure (dim)
L	= reinforcement length (ft)
L_e	= embedment length in the resisting zone (ft)
p_f	= probability of failure (dim)
Q	= random variable representing load
Q_n	= nominal load (lb)
Q_{ni}	= a specific nominal load component type (i.e., vertical and lateral earth loads, surcharges and vehicle live loads for MSE walls) (lb)
R	= random variable representing resistance
R_c	= reinforcement coverage ratio = b/S_h (dim)
R_n	= nominal or ultimate resistance (lb)
S_h	= horizontal spacing of reinforcement (ft)
S_t	= spacing of transverse bars
S_v	= vertical spacing of reinforcement (ft)
t	= thickness of transverse bar (in)
T_{max}	= maximum tensile load in reinforcement (lb)
α	= scale effect correction factor = 1 (dim)
β	= reliability index (dim)
β_t	= target reliability index (dim)
γ_i	= load factor applicable to a specific load component i (dim)
γ_s	= total unit weight (pcf)
$\bar{\sigma}_h$	= horizontal effective stress (psf)
$\bar{\sigma}_v$	= vertical effective stress (psf)
ϕ	= resistance factor for a particular failure mode and limit state (lb)
ϕ_s	= mobilized angle of friction of backfill soil in reinforced zone (°)



1. Introduction

Since their introduction about 40 years ago, MSE walls have been proportioned to satisfy safety criteria against soil failure by sliding, bearing and overturning (i.e., external stability), and to satisfy safety criteria against structural failure by pullout or rupture of the reinforcements in the reinforced soil mass (i.e., internal stability) and at the connection between the reinforcement and the facing. In the *LRFD Specifications* (AASHTO, 2007), these safety criteria are met by ensuring that the sum of the factored resistances exceeds the sum of the factored load effects. Analytically this is demonstrated in LRFD by:

$$\sum \gamma_i Q_{ni} \leq \phi R_n \quad \text{Eq. 1}$$

where:

γ_i	= load factor applicable to a specific load component i (dim)
Q_{ni}	= a specific nominal load component type (i.e., vertical and lateral earth loads, surcharges and vehicle live loads for MSE walls) (lb)
$\sum \gamma_i Q_{ni}$	= total factored load for the load group applicable to the limit state being considered (lb)
ϕ	= resistance factor for a particular failure mode and limit state (dim)
R_n	= nominal or ultimate resistance (lb)

A limit state is a condition in which a combination of one or more loads just equals the available resistance, so that the structure is at incipient failure defined by a prescribed failure criterion. Each failure criterion is represented by an equation having the general form of Eq. 1.

The load and resistance factors in Eq. 1 are used to account for material variability, uncertainty in magnitude and application of the applied loads, design model prediction uncertainty, and other sources of uncertainty. The objective in LRFD is to ensure that for each limit state the available factored resistance (i.e., ϕR_n) is at least as large as the total factored load effects (i.e., $\sum \gamma_i Q_{ni}$).

Beginning with the Interims to the 1991 AASHTO Standard Specifications for Highway Bridges (*Standard Specifications*), the *Standard Specifications* permitted the maximum load at each reinforcement level to be computed using the:

- Coherent Gravity Method;
- Tieback Wedge Method; or
- Structure Stiffness Method

Then in the late 1990s, Technical Committee T-15 on Substructures and Retaining Walls of the AASHTO Subcommittee on Bridges and Structures decided to incorporate then new developments in the internal stress design of MSE walls with the previous methodology, and to adapt these developments in the AASHTO design codes for MSE wall design. For this development, data from full-scale MSE wall case histories were compiled and analyzed to evaluate the existing methods for calculating reinforcement stresses, and to modify or develop a new approach for estimating reinforcement stresses. This development led to the Simplified Method (Allen, et al., 2001) which was included in the 1999 interims to the *Standard Specifications* and the *LRFD Specifications*.



Article 11.10.6.2.1 of the *LRFD Specifications* (2007) requires that the maximum load in reinforcements be calculated using the Simplified Method approach along with the prescribed resistance factors calibrated for the method. So while the LRFD Specifications allow “other widely accepted and published design methods” to be used “for calculation of reinforcement loads”, alternative methods (e.g., Coherent Gravity) are permitted only “if the wall designer develops method-specific resistance factors for the method employed”. Therefore, the objective of the study is to develop resistance factors for the internal stability design of metallicity reinforced MSE walls using the Coherent Gravity Method.

2. Database

D’Appolonia compiled a worldwide database of selected, well documented MSEW case studies from the literature and through personal communications. The database includes 17 full-scale metallicity reinforced MSE walls (22 wall sections) as summarized in Table 1. Five of the walls are reinforced using steel grids and 12 of the walls are reinforced using steel strips. The walls were constructed between 1972 and 1998. The cross sections of the reinforcements for the wall sections are rectangular except for three sections which are trapezoidal. Except for the Guildford Bypass Wall (Profiles A and B), all of the walls using steel strip reinforcements were constructed by the Reinforced Earth Company (RECO). All of the walls using bar mat reinforcements were constructed by VSL. All of the walls using welded wire reinforcements were constructed by Hilfiker Retaining Walls. The wall sections were instrumented to evaluate their field performance and measure in-situ stresses and deformations of steel reinforcements due to static earth loads during and for short-term periods after construction. For this study, our interest focused on deformations and tensile stresses measured on the steel reinforcements. Other field measurements such as soil vertical and horizontal pressures are used to generally check the validity of soil backfill properties used in the design. Wall geometries, backfill properties, cross section and spacing of steel elements, and maximum measured tensile loads are summarized in Tables A-1 to A-3 in Appendix A.

Some of the walls included in the database represent special cases. They include:

1. Guildford Bypass Wall Sections: These wall sections were constructed using the York method and were heavily reinforced with smooth steel strips. The wall sections have a special hexagonal facing which is commercially uncommon and the reported measured angle of internal friction is over 50° , which is very high for granular reinforced backfill. For this study we used the mobilized angle of friction (35°) reported by Murray and Hollinghurst (1986) to calculate the reinforcement loads.
2. Minnow Creek Wall: This structure supports a bridge abutment that bears on steel H-piles that extend through the wall cross section. The piles are surrounded by corrugated pile to isolate the piles from the wall. As such there is no interference between the studied wall section and the bridge foundations (Runser, et al., 2001).
3. Houston Wall 17: MSE walls were constructed back-to-back to retain an approach to a highway bridge. Sampaco (1995) indicated that there was no overlap of soil reinforcements between the two walls at the studied section.



Therefore, given the particular features described in the previous list, we believe that the data provided from these wall sections do not represent outliers within the database, and can be acceptably included with data from the other walls in the calibration analysis.

2.1 Database Statistics

The statistical characteristics in the database include information regarding wall geometries, the engineering properties of the reinforced soil backfill, and reinforcement type, dimensions and spacing. Tables 2 through 4 summarize the maximum, average and minimum of different parameters of the database. Table 2 indicates that wall heights in the database vary between 12 feet and 62 feet. For these walls, the ratio of the reinforcement length to the wall height (L/H) varies between 0.38 and 1.79. AASHTO (1999) specifies $L/H \geq 0.7$, however the code permits L/H as low as 0.63 for high structures where $H \geq 40$ feet. The angle of friction of the backfill soils for walls in the database varies between 30° and 44° . For the Simplified Method, AASHTO (1999) allows a maximum backfill friction angle of 34° , unless the backfill is tested for frictional strength using triaxial or direct shear laboratory methods. Tables 3 and 4 summarize the range and the average of cross section and spacing of steel strips and grids. The two types of steel reinforcement have similar average vertical spacing of about 2.2 feet.

3. Load-Resistance Calculation

The maximum tension load, pullout resistance and rupture resistance on the steel reinforcement were calculated using the Coherent Gravity Method as defined by the *Standard Specifications* (1996). The internal forces are a function of the position and strength of steel reinforcement within the reinforced soil mass. The nominal tension load ($Q_n = T_{\max}$) in a steel reinforcement element is calculated as:

$$Q_n = T_{\max} = \bar{\sigma}_h A = K \bar{\sigma}_v A \quad \text{Eq. 2}$$

where:

- $\bar{\sigma}_h$ = horizontal effective stress (psf)
- A = tributary wall area for a steel strip or grid (sf)
- K = coefficient of lateral earth pressure (dim)
- $\bar{\sigma}_v$ = vertical effective stress (psf)

The Coherent Gravity Method assumes an at rest, $K = K_o$, at the top of a wall, as shown on Figure 1, transitioning to a Rankine active earth pressure coefficient, K_a at a depth of 20 feet and lower depths.





Table 1. Summary of Wall Sections

Catalog Number	Wall Name	Wall Type	Steel Type ⁽¹⁾	Construction Year	Location	Section Type	Reference
S1	UCLA Wall	RECO	Smooth steel strips	1974	CA, USA	Rectangular	Richardson, et al. (1977)
S2	Vicksburg WES Wall	RECO	Smooth steel strips	1976	MS, USA	Rectangular	Al-Hussaini and Perry (1978)
S3	Guildford Bypass Wall, Profile A	York	Smooth steel strips	1981	UK	Rectangular	Murray and Hollinghurst (1986); Hollinghurst and Murray. (1986)
S4	Guildford Bypass Wall, Profile B	York	Smooth steel strips	1981	UK	Rectangular	
S5	Algonquin Wall 1	RECO	Ribbed steel strips	1988	IL, USA	Rectangular	Christopher (1993)
S6	Waltham Wall	RECO	Mild ribbed steel strips	1981	UK	Trapezoidal ⁽²⁾	Murray and Farra (1990)
S7	Asahigaoka Wall	RECO	Smooth steel strips	1982	Japan	Trapezoidal ⁽²⁾	Bastick (1984)
S8	Lille Wall	RECO	Smooth stainless steel strips	1972	France	Rectangular	Bastick (1984)
S9	Fremersdorf Wall	RECO	Ribbed steel strips	1980	Germany	Rectangular	Bastick (1984)
S10	Minnow Creek Wall	RECO	Ribbed steel strips	1998	IN, USA	Rectangular	Runser, et al. (2001)
S11	Gjovik Wall	RECO	Ribbed steel strips	1990	Norway	Rectangular	Allen, et al. (2001)
S12	Ngauranga Wall	RECO	Ribbed steel strips	1985	New Zealand	Trapezoidal ⁽²⁾	Boyd (1993)
S13	Bourron Marlotte Wall	RECO	Ribbed steel strips	1993	France	Rectangular	Bastick et al. (1993)
S14	Bourron Marlotte Wall	RECO	Ribbed steel strips	1993	France	Trapezoidal ⁽²⁾	Bastick et al. (1993)
BM1	Hayward Wall, Section 1	VSL	Bar mat	1981	CA, USA	Rectangular	Neely (1993)
BM2	Hayward Wall, Section 2	VSL	Bar mat	1981	CA, USA	Rectangular	Neely (1993)
BM3	Cloverdale Wall	VSL	Bar mat	1988	CA, USA	Rectangular	Jakura (1988)
BM4	Algonquin Wall 3	VSL	Bar mat	1988	IL, USA	Rectangular	Christopher (1993)
BM5	Algonquin Wall 4	VSL	Bar mat	1988	IL, USA	Rectangular	Christopher (1993)
BM6	Algonquin Wall 5	VSL	Bar mat	1988	IL, USA	Rectangular	Christopher (1993)
WW1	Rainier Seattle Wall	Hilfiker	Welded wire	1985	WA, USA	Rectangular	Anderson, et al. (1987)
WW2	Houston Wall 17	Hilfiker	Welded wire	1991	TX, USA	Rectangular	Sampaco (1995)

⁽¹⁾ Steel reinforcements of wall sections are galvanized except for Rainier Seattle wall.

⁽²⁾ Trapezoidal sections typically use shorted reinforcements in the lower portion of the wall except for Waltham wall where longer reinforcements were used in the upper portion of the wall.

Table 2. Statistical Summary of Wall Geometries and Backfill Soil Properties

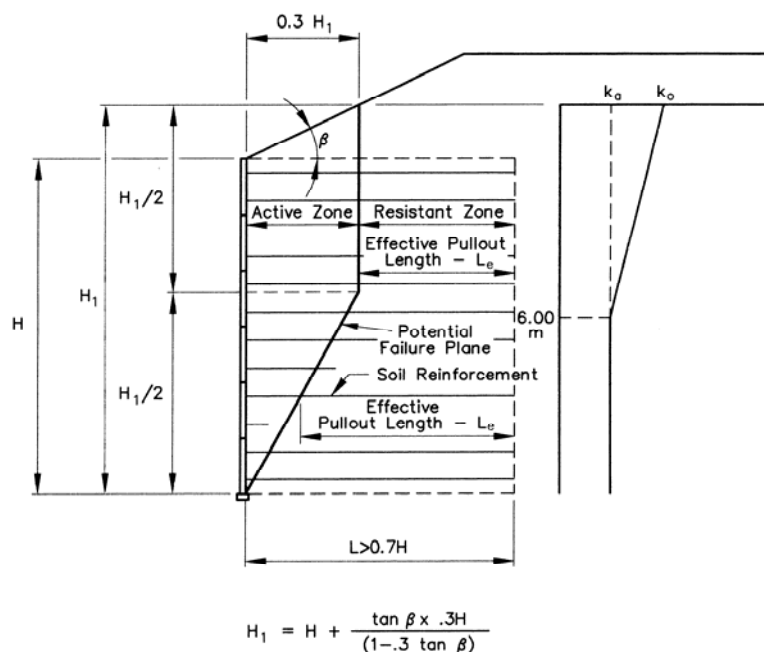
Parameter	Wall Height, H (ft)	Reinforcement Length, L (ft)	L/H (dim)	Total Soil Unit Weight, γ_s (pcf)	Mobilized Angle of Friction, ϕ_s (°)
Min	12.0	10.0	0.38	100.0	30.0
Max	62.0	49.2	1.79	144.0	44.0
Average	30.8	24.0	0.81	124.3	36.8

Table 3. Statistical Summary of Steel Strip Reinforcement Cross Section and Spacing

Parameter	Vertical Spacing S_v (ft)	Horizontal Spacing S_h (ft)	Width b (in)	Thickness, t (in)	$R_c = b/S_h$ (dim)
Min	0.98	1.02	1.57	0.025	0.05
Max	2.50	3.28	4.00	0.591	0.20
Average	2.20	2.26	2.71	0.214	0.11

Table 4. Statistical Summary of Steel Grid Reinforcement Cross Section and Spacing

Parameter	Longitudinal Steel					Transverse Steel	
	S_v (ft)	S_h (ft)	Diameter (in)	b (ft)	$R_c = b/S_h$ (dim)	Diameter (in)	S_t (ft)
Min	1.50	0.50	0.239	0.5	0.28	0.211	0.75
Max	2.50	6.73	0.507	4.0	1.00	0.375	2.00
Average	2.22	4.10	0.377	2.0	0.56	0.333	1.73

**Figure 1. Earth Pressure Coefficients for MSE Walls with Inextensible Reinforcement (AASHTO 1996)**

The nominal pullout resistance ($T_{po} = P_r$) of a steel reinforcement element is given by:

$$T_{po} = P_r = F^* \alpha \bar{\sigma}_v L_e C R_c S_h \quad \text{Eq. 3}$$

where:

- F^* = pullout resistance factor, which is a function of passive and frictional resistance of reinforcement (see Table 5) (dim)
 α = scale effect correction factor = 1 (dim)
 L_e = embedment length in the resisting zone (ft)
 C = effective unit perimeter of reinforcement = 2 (dim)
 R_c = reinforcement coverage ratio (dim)
 S_h = horizontal spacing of reinforcement(ft)

Table 5. Design Values for F^* (AASHTO, 1999)

Reinforcement Type	Top of Wall	Depth of 20 Feet and Below
Smooth Strips	0.4	0.4
Ribbed Strips	$1.2 + \log(C_u) \leq 2.0$	$\tan(\text{Angle of Friction})$
Grids	$20 (t/S_t)$	$10 (t/S_t)$

Notes: C_u = uniformity coefficient of backfill; t = thickness of transverse bar
 S_t = spacing of transverse bars

The nominal rupture resistance ($T_{po} = R_r$) of a steel reinforcement element is given by:

$$T_{po} = R_r = F_y A_c \quad \text{Eq. 4}$$

where:

- F_y = steel yield strength (ksi)
 A_c = steel area corrected for corrosion (in²)

The nominal tension loads, pullout resistances and rupture resistances of steel reinforcing of different wall sections in the database were calculated using Eqs. 2, 3 and 4. The loads and resistances were calculated at the end of construction assuming no corrosion and 75 years of service life considering the effects of corrosion using the AASHTO (2007) corrosion model as the basis for loss of reinforcement cross section. The AASHTO metal-loss model defines the rates at which first zinc, then steel, will be lost from the MSE reinforcement section. For each exposed surface, these rates are:

- Loss of zinc (first 2 years) 15 $\mu\text{m}/\text{yr}$ (0.59 mil/yr)
- Loss of zinc (to depletion) 4 $\mu\text{m}/\text{yr}$ (0.16 mil/yr)
- Loss of steel (after zinc depletion) 12 $\mu\text{m}/\text{yr}$ (0.47 mil/yr)

Using the specified 86 μm (3.39 mil) thickness of zinc (AASHTO, 2007), the calculated life of the zinc is 16 years, followed by 59 years of steel loss of strength before the 75 year design life is reached.

Comparisons between the calculated nominal tension load and pullout resistance without corrosion are shown in Figure 2 for steel strips and in Figure 3 for steel grids. Comparisons



between calculated nominal tension load and rupture resistance without corrosion are shown in Figure 4 for steel strips and Figure 5 for steel grids. Summaries of the ratio of nominal resistance to load (i.e., factor of safety) for pullout and rupture, with and without corrosion, are presented in Table 6 for steel strips and in Table 7 for steel grids. Table 6 shows average safety factors of 3.39 and 22.39 against pullout and rupture for corroded steel strips. Table 7 shows average safety factors of 7.02 and 8.75 against pullout and rupture for corroded steel grids. The FHWA guidelines (2001) specify using a safety factor of 1.50 for steel pullout in Allowable Stress Design (ASD). Also, it specifies rupture safety factors of 1.82 and 2.08 for steel strip and steel grid, respectively. Therefore, the Coherent Gravity Method provides more than twice the pullout capacity and more than quadruple the rupture capacity specified by the FHWA guidelines.

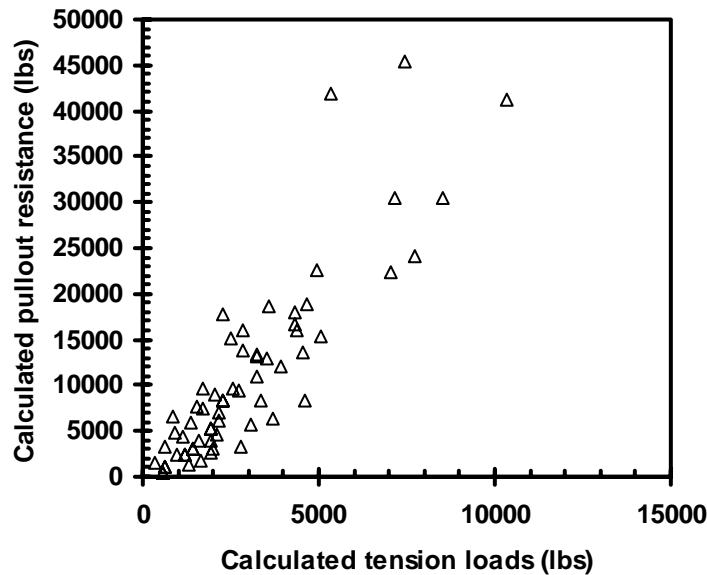


Figure 2. Comparison Between Calculated Loads and Pullout Resistance for Steel Strips Without Corrosion

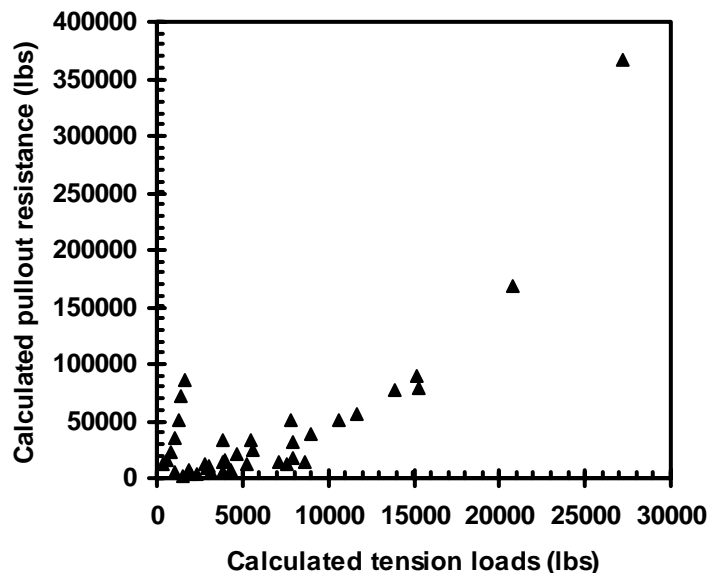


Figure 3. Comparison Between Calculated Loads and Pullout Resistance for Steel Grids Without Corrosion



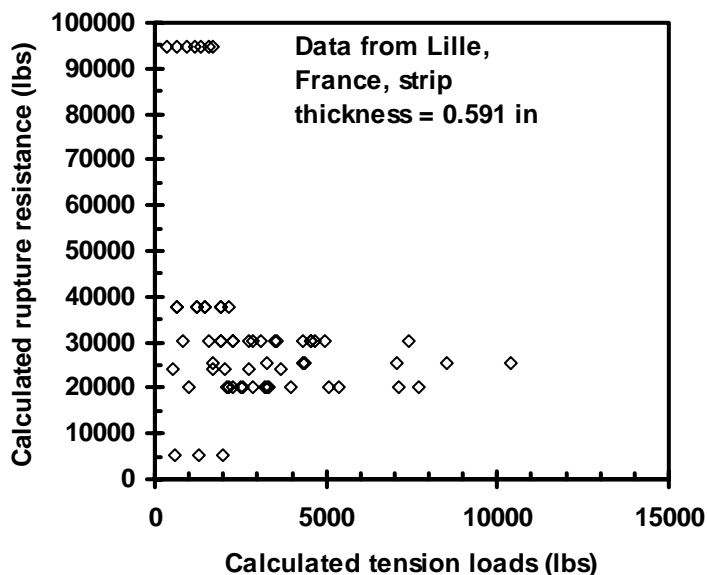


Figure 4. Comparison Between Calculated Loads and Rapture Resistance for Steel Strips Without Corrosion

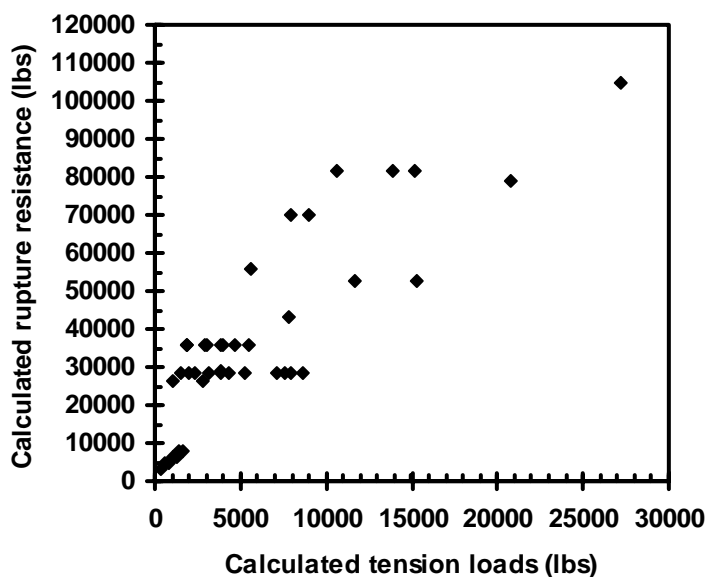


Figure 5. Comparison Between Calculated Loads and Rapture Resistance for Steel Grids Without Corrosion

Table 6. Ratio of Nominal Resistance Versus Load for Steel Strips

Statistical parameter	Corrosion Ignored		Corrosion Considered	
	Pullout (Resistance/Load)	Rapture (Resistance/Load)	Pullout (Resistance/Load)	Rapture (Resistance/Load)
Min	0.88	2.44	0.00	0.00
Max	7.94	284.19	7.85	284.19
Average	3.48	24.58	3.39	22.39

Note: Corrosion of the stainless steel reinforcements of Lille wall, France was ignored because stainless steel corrodes at a much lower rate than that of a regular steel.



Table 7. Ratio of Nominal Resistance Versus Load for Steel Grids

Statistical Parameter	Corrosion Ignored		Corrosion Considered	
	Pullout (Resistance/Load)	Rupture (Resistance/Load)	Pullout (Resistance/Load)	Rupture (Resistance/Load)
Min	1.27	3.29	1.18	2.82
Max	53.08	24.08	45.66	18.82
Average	10.07	8.32	8.75	7.02

4. Calibration Using Monte Carlo Analysis

Calibration of the Coherent Gravity Method herein is conducted using the Level II probabilistic analysis method described in Allen, et al. (2005). The goal of a Level II analysis for the internal stability of MSE reinforcements is to develop factors that decrease the nominal resistance of reinforcements to give a design with an acceptable and consistent probability of failure. To accomplish this, a limit state equation is developed that incorporates and relates together all of the variables that affect the potential for failure of the reinforcements for each limit state (i.e., rupture and pullout). The parameters of load and resistance are considered as random variables, with the variation modeled using the available statistical data.

The required steps needed to conduct the calibrations are:

- *Step 1* – Develop a limit state equation for each failure mechanism (i.e., rupture and pullout) so that the correct random variables are considered. The limit state equations include all the parameters that describe the failure mechanism and that are used to conduct a deterministic design of metallic MSE wall reinforcements.
- *Step 2* – Statistically characterize the data upon which the calibration is based. The key parameters include the mean, \bar{x} , standard deviation, σ , coefficient of variation, $COV = \bar{x}/\sigma$, and bias factor, $\lambda = \text{measured value}/\text{predicted value}$.
- *Step 3* – Select a target reliability value based on the margin of safety implied in MSE wall designs for internal stability considering the need for consistency with reliability values used in developing the *LRFD Specifications*.
- *Step 4* – Determine resistance factors for reinforcement rupture and pullout using reliability theory consistent with the selected target reliability.

A more detailed description of each step is presented in the following sections.

Step 1 – Develop Limit State Equations

The limit state equation is given as:

$$g = R - Q \geq 0 \quad \text{Eq. 5}$$

where:

g = random variable representing the safety margin
R = random variable representing resistance
Q = random variable representing load



The factored values for load and resistance are calculated from Eq. 5 by setting the left side of the relationship equal to zero (i.e., the point at which the limit state is just reached). Generally, the resistance required is calculated knowing the load applied, and the resistance is increased to be greater than the load by a combination of load and resistance factors so that failure due to inadequate resistance is unlikely. What is important to understand here is that the nominal values of load and resistance must be properly related to one another through the use of the design equation that corresponds to the limit state function being considered. Thus for a given nominal value of the load Q_n , the value of R_n must be greater than Q_n by some factor that is a function of the load and resistance factors used for design.

The magnitude of the load and resistance factors, and the difference between R and Q , are determined such that the probability of failure, P_f , that $Q > R$ is acceptably small. Figure 6 illustrates this principle, in this case for normal distributions for load and resistance. In the left side of Figure 6, failure is represented by the zone where the load and resistance distributions overlap, and the area under the curve equals P_f . Thus the idea behind calibration is to separate the load and resistance distributions far enough apart so that the P_f is acceptably low. (In terms of allowable stress design [ASD] principles, more overlap between the Q and R distributions represents a lower factor of safety while a smaller overlap represents a higher factor of safety.) The right side of Figure 6 is an alternative representation of the Q and R distributions to the left, but the distributions are combined in the right side of the figure to represent the limit state function, $R - Q$. This distribution, which is called the cumulative distribution function, or CDF, combines all the attributes of the separate Q and R distributions into a single form that is more amenable to mathematical processing. Using the CDF, the level of safety is represented by the distance the mean value is offset to the right of the origin. Thus, if the CDF is offset more to the right, the margin of safety against failure will increase and the P_f will decrease. Conversely, shifting the CDF to the left will reduce the margin of safety and increase the P_f . Using the CDF, the P_f is typically represented by the reliability index, β , which represents the number of standard deviations of the mean of $R - Q$, or $\bar{R} - \bar{Q}$, to the right of the origin, as shown in the right hand figure. Here $\beta = 1/\text{COV}$ for the limit state function, $g = R - Q$, and is related to P_f when $R - Q < 0$.

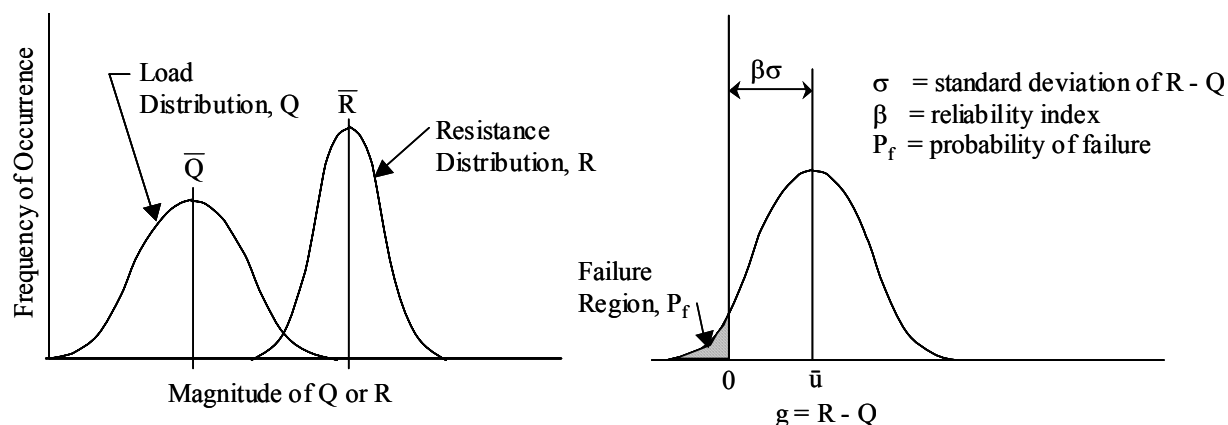


Figure 6. Probability of Failure and Reliability Index

Using Eqs. 2, 3 and 5, the limit state equation for pullout of steel reinforcement using the Coherent Gravity Method is:

$$g = R - Q = \phi F^* \alpha \bar{\sigma}_v L_e C R_c S_h - \gamma K \bar{\sigma}_v A \geq 0 \quad \text{Eq. 6}$$



Using Eqs. 2, 4 and 5, the limit state equation for rupture of steel reinforcements using the Coherent Gravity Method is:

$$g = R - Q = \phi F_y A_c - \gamma K \bar{\sigma}_v A \geq 0 \quad \text{Eq. 7}$$

Step 2 – Statistically Characterize the Performance Data

For this calibration, the statistical characterization focuses on the prediction of peak loads relative to the peak loads actually measured in the MSE structures summarized previously. Measured peak loads from instrumented structures are summarized in Table A-2, and predicted loads are calculated using Eq. 2. Figure 7 compares the maximum measured and calculated tension loads for steel strips at the end of construction (i.e., no corrosion). Figure 7 shows generally good agreement between measured and predicted loads up to a load envelope of about 6000 lbs, but that beyond 6000 lbs the relationships are more scattered. Figure 8 compares the maximum measured and calculated tension loads for steel grids at the end of construction. Figure 8 shows general agreement between measured and predicted loads except for few points.

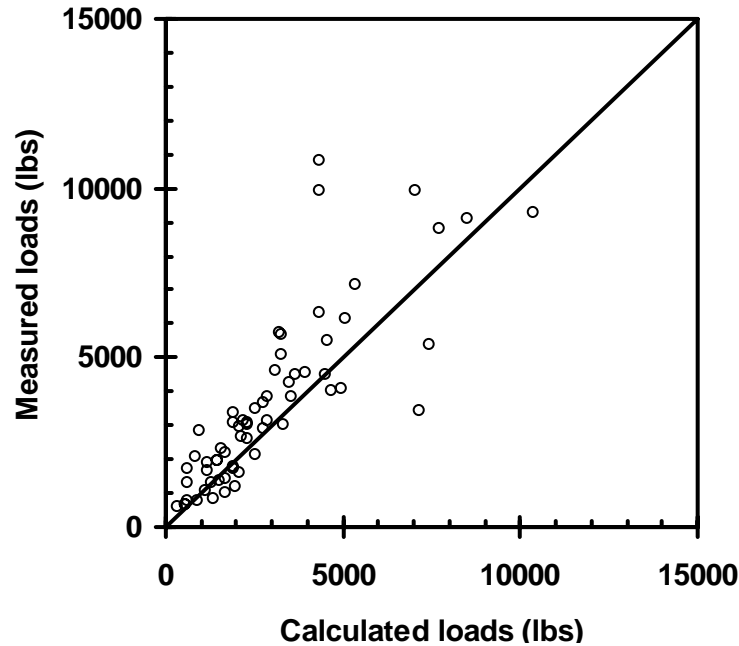


Figure 7. Comparison Between Measured and Calculated Tension Loads for Steel Strips

The load bias is determined as the ratio of the measured to the predicted loads. Statistical parameters (mean and COV) of measured and predicted loads, and predicted pullout and rupture resistances of steel strips and steel grids are summarized in Tables 8 and 9, respectively. The bias of pullout resistance is determined using a database reported by D'Appolonia (1999). The bias of rupture resistance is modeled as a normal distribution (Buonopane, et al., 2003) with $\bar{x} = 1.05$ and $COV = 0.10$.

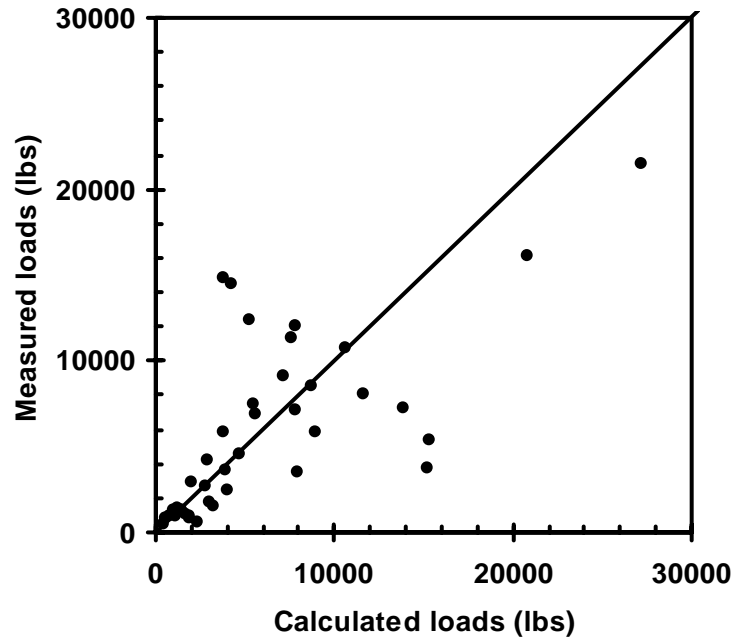


Figure 8. Comparison Between Measured and Calculated Tension Loads for Steel Grids

Table 8. Statistical Properties of Steel Strip Data Sets

Variable	Mean	COV	Source
Predicted Load	2951 lbs.	0.717	This Study
Measured Load	3575 lbs.	0.710	
Load Bias	1.294	0.386	
Predicted Pullout Resistance (No Corrosion)	10953 lbs.	0.927	
Predicted Pullout Resistance (With Corrosion)	10752 lbs.	0.940	
Predicted Rupture Resistance (No Corrosion)	33865 lbs.	0.678	
Predicted Rupture Resistance (With Corrosion)	29667 lbs.	0.819	
Pullout Bias	2.28	0.605	D'Appolonia (1999)
Rupture Bias	1.05	0.10	Buonopane, et al. (2003)

Table 9. Statistical Properties of Steel Grid Data Sets

Variable	Mean	COV	Source
Predicted Load	6031 lbs.	0.967	This Study
Measured Load	5684 lbs.	0.909	
Load Bias	1.084	0.680	
Predicted Pullout Resistance (No Corrosion)	39726 lbs.	1.575	
Predicted Pullout Resistance (With Corrosion)	36049 lbs.	1.603	
Predicted Rupture Resistance (No Corrosion)	37360 lbs.	0.656	
Predicted Rupture Resistance (With Corrosion)	32238 lbs.	0.676	
Pullout Bias	1.318	0.387	D'Appolonia (1999)
Rupture Bias	1.05	0.10	Buonopane, et al. (2003)



Normal and lognormal statistical distributions are typically used in LRFD calibrations (e.g., D'Appolonia, 1999). Using a Monte Carlo analysis requires pre determination of the statistical distribution of the data. The Shapiro-Wilk test for normality (W test) can be applied on the collected data of loads, resistances and biases to check the goodness of fit of each data set to a normal distribution (Shapiro and Wilk 1965). The test statistic W ranges from $0 < W \leq 1$, where 0 indicates no normality and 1 indicates normality. The W test was performed using Lumenaut (2007) software, Version 3.4.21, which is compatible with Microsoft Excel. The software is convenient to use because the modules for Lumenaut appear on the Tools menu of Excel. The normality W test results of the steel strip and steel grid data are shown in Tables 10 and 11, respectively.

Table 10. Normality W Test for Steel Strip Data Biases

Variable	Goodness to Fit Normal Distribution (W test result)	Goodness to Fit Lognormal Distribution (W test result)
Load bias	0.90	0.98
Pullout bias	0.81	0.96

Table 11. Normality W Test for Steel Grid Data Biases

Variable	Goodness to Fit Normal Distribution (W Test Result)	Goodness to Fit Lognormal Distribution (W Test Result)
Load bias	0.77	0.97
Pullout bias	0.93	0.99

To check the lognormality of a data set, Singh, et al. (1998) stated that a data set is lognormally distributed if the log-transformed data are normally distributed. Therefore, all of the data sets were log-transformed and then tested using the W test statistic. The lognormality W test results are shown in Table 10 for the steel strips and Table 11 for the steel grids. The W test results indicate that using the lognormal distribution for the load bias and pullout bias is appropriate for the calibration of the steel strip and the steel grid data.

Step 3 – Select Target β

The value of β implied by the various design methods to evaluate a given limit state will vary depending on the design method being evaluated, the redundancy of structural elements, and the consequences of failure. This variation in β occurs because each design method has different statistics (i.e., mean, standard deviation, distribution type, bias in the selection of material properties, and bias in the design equation used). For example, previous studies to assess the reliability inherent in ASD foundation and retaining wall design practice (e.g., Barker, et al., 1991; D'Appolonia, 1999; Paikowsky, et al., 2005; Allen, et al., 2005) have reported that β ranges from about 3.5 to 2.3 depending on the type of structure. For the example calibration for pullout of steel grid presented in Allen, et al. (2005), $\beta_T = 2.3$ was used based on recommendations presented in D'Appolonia (1999) to reflect the redundancy of structural elements in the MSE wall reinforced soil mass used for the analyses. Those analyses were, however, conducted using the Simplified Method. For the calibration analysis herein, β represents the output of the Monte Carlo analysis and is compared to these ranges for acceptability. Also, β obtained using the Monte Carlo analysis is validated against β using an approximate closed-form solution. The results are discussed in Step 4.



Step 4 – Determine Resistance Factors

Using the limit state equation from Step 1 and the statistical properties compiled from Step 2, the resistance factor can be estimated through iteration to produce the desired magnitude for β (Step 3). Estimates of β can be accomplished using exact or approximate closed-form solutions, a graphical approach referred to as the Rackwitz-Fiessler procedure, or Monte Carlo simulation. For the proposed calibrations, the Monte Carlo simulation method is used because the approach is more adaptable and sufficiently rigorous to deal with the variability of the available data, and the method has become the preferred approach for calibrating load and resistance factors for the *LRFD Specifications*.

The Monte Carlo method is simply a technique that utilizes a random number generator to extrapolate the CDF values for each random variable where the CDF is characterized by the mean, standard deviation, and the type of CDF function (e.g., normal or lognormal). This extrapolation of the CDF plots makes estimating β possible because in most cases the quantity of measured data is inadequate to reliably estimate β . As the extrapolated CDF plots are created, the limit state function is used to relate the CDF plots together as values of each random variable are generated. The analyses are conducted using the Lumenaut software, however the step-by-step procedure for Monte Carlo simulations presented in Allen, et al. (2005) can be performed using Excel spread sheets and built in functions.

4.1 A Monte Carlo Simulation Example

An example Monte Carlo simulation run input and output report using Lumenaut software is shown in Figure 9. The data in the figure represent a Monte Carlo analysis to determine β for pullout of steel strips at the end of a structure design life (considering corrosion). The mean and standard deviation of the load bias (Table 8) are the input for the load. The mean and standard deviation of the pullout resistance bias (Table 8) are the input for the resistance. As shown in Table 10, the distribution of the biases is lognormal. The random numbers for the limit state function, g , (Eq. 6) are generated using the statistical properties of the inputs from Table 8 for load and resistance, a load factor, $\gamma = 1.35$ (AASHTO 2007 for static earth pressure loads), and a resistance factor, $\phi = 0.9$. For each Monte Carlo run, including the one shown in Figure 9, 10000 iterations (i.e., g 's) are generated. The iteration results are summarized in the form of a histogram and corresponding intervals are summarized in a table. A spread sheet, including the actual 10000 iterations, is also generated as an output. The g values are then sorted and ranked in an ascending order. The cumulative probability at each g , $p(g)$, is calculated as (g rank/(10000+1)). Then the standardized normal value (z) of a $p(g)$ is calculated using the NORMSINV function in Microsoft Excel (where $z = \text{NORMSINV}[p(g)]$). The reliability index, β , is equal to $(-z)$ at $g = 0$. Figure 10 shows the standardized normal variable (z) versus randomly generated g for the above run, and $\beta = 2.38$ corresponding to $p_f = 8.7\text{E-}03$.

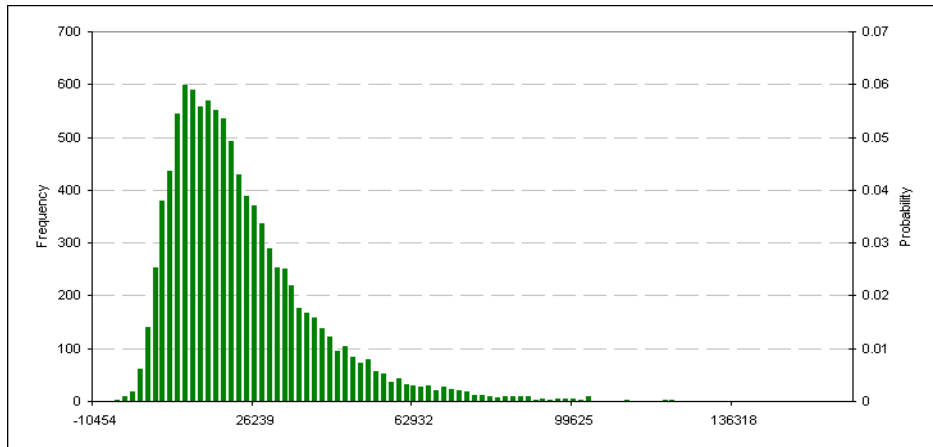
The numerical results for the simulation example are:

No. of iterations of Monte Carlo simulation	= 10,000
Ascending rank of ($g = 0$)	= 87
$p_f =$ Cumulative probability at ($g = 0$), $p(g = 0) = (87/10001)$	= 8.7 E-03
Standardized normal variable, z at ($g = 0$) = NORMSINV [$p(g = 0)$]	= -2.38
Reliability index, $\beta = -z$	= 2.38



Lumenaut Simulation Report

Output Cell: MC Input!\$B\$26 Workbook: P-S-L-0.9-corrosion.xls
 Output Name: g Date: 11-Oct-07
 Iterations: 10000 Time: 1:42:52 PM



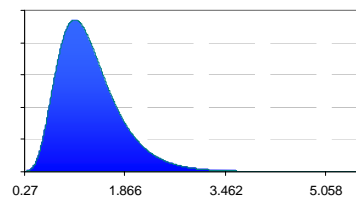
Percentile	Min to Max
0%	-12200.86329
10%	5864.948739
20%	9308.47782
30%	12154.56238
40%	15264.68972
50%	18379.38731
60%	22071.82001
70%	26614.55641
80%	32801.09411
90%	43246.27833
100%	162527.6084

Percentile	Max to Min
0%	162527.6084
10%	43246.27833
20%	32801.09411
30%	26614.55641
40%	22071.82001
50%	18379.38731
60%	15264.68972
70%	12154.56238
80%	9308.47782
90%	5864.948739
100%	-12200.86329

Mean	22197.9601
Median	18377.66283
Mode	5.50244E+21
Stand. Deviation	16418.7504
Variance	269575364.7
Mean Std. Error	164.187504
Range	174728.4717
Range Min	-12200.86329
Range Max	162527.6084
Skewness	1.664016357
Kurtosis	4.572478427

Lumenaut Simulation Input

Cell Name: Load bias
 Cell: MC Input!\$B\$17
 Distribution: Lognormal
 Mean: 1.314
 Stand. Dev.: 0.502
 Min: 0.27
 Max: 5.59



Cell Name: Pullout bias
 Cell: MC Input!\$B\$7
 Distribution: Lognormal
 Mean: 2.28
 Stand. Dev.: 1.38
 Min: 0.2
 Max: 19.34

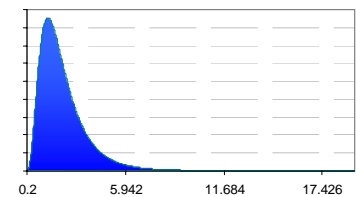


Figure 9. Monte Carlo Simulation Example Showing Input and Output Report for Pullout Resistance of Steel Strips Considering Corrosion ($\gamma = 1.35$, $\phi = 0.9$)



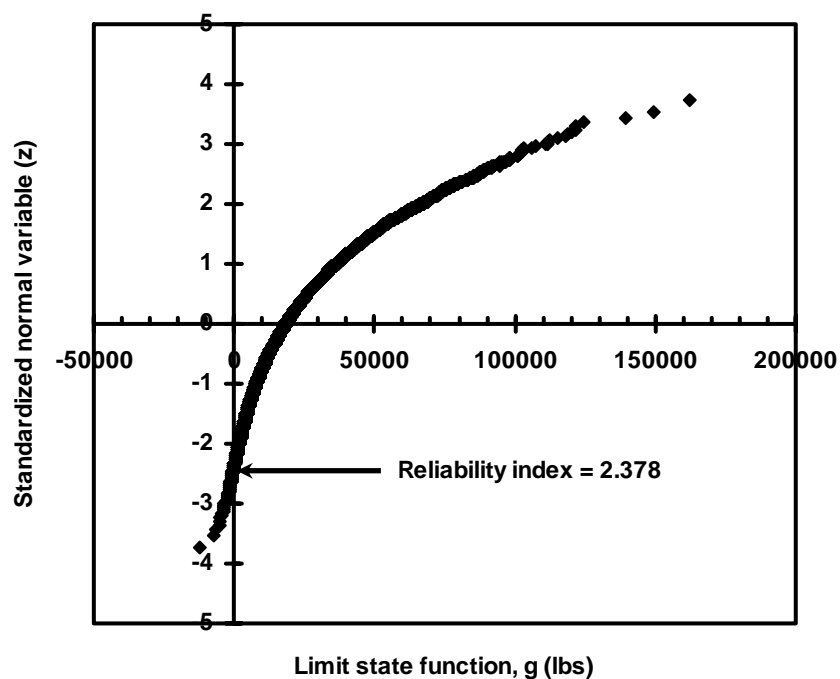


Figure 10. Monte Carlo Analysis Results for Pullout Resistance of Steel Strips Considering Corrosion ($\gamma = 1.35$, $\gamma = 0.9$)

4.2 Monte Carlo Simulation Analyses

Similar Monte Carlo analyses were performed to calibrate the pullout and rupture resistances of steel strips and steel grids. The limit state function, g , depends on three variables (i.e., γ , ϕ and β). For all of the analyses, $\gamma = 1.35$ corresponding to static earth pressure loads was adopted. For each analysis, a value ϕ was assumed and the corresponding p_f and β were determined. A statistical distribution (normal or lognormal) of a data set was adopted according to the goodness of fit test (W test), as described in *Step 2*. The Monte Carlo simulation results are summarized in the following sections.

4.3 Calibration of Pullout Resistance

For calibration of pullout resistance, the load factor was fixed at $\gamma = 1.35$, and values of ϕ ranging from 0.65 to 0.90 were selected based on previous AASHTO calibrations for static loading of soil reinforcements. The current *LRFD Specifications* (2007) prescribes $\phi = 0.9$ for the pullout resistance of metallic reinforcement. Therefore, ϕ values of 0.70 and 0.90 were adopted for the analyses.

4.3.1 Calibration of Pullout Resistance for Steel Strips

The pullout resistance of steel strips was calibrated using a lognormal distribution for the load and resistance data based on W test results. Three Monte Carlo simulation analyses were performed and the results are summarized in Table 12. The Monte Carlo simulation input and output reports are presented in Appendix B. For $\phi = 0.7$ at the end of construction (no



corrosion), the Monte Carlo simulation results in a $p_f = 2.3E-03$ and $\beta = 2.83$ (see Table 12 and Figure 11). For $\phi = 0.9$ at the end of construction (no corrosion), the Monte Carlo simulation resulted in $p_f = 8.6E-03$ and $\beta = 2.38$ (see Table 12 and Figure 12). For $\phi = 0.9$ at the end of a structure lifetime (considering corrosion), the results were discussed previously (see Figures 9 and 10). Considering the steel corrosion over the lifetime (75 years) of a structure has resulted in a negligible decrease of β (about 0.2%) and a minor increase in p_f (about 1.2%). The resulted β s are within the practical range (3.5 to 2.3) reported for previous LRFD calibrations.

Table 12. Calibration Results of Pullout Resistance for Steel Strips

γ	ϕ	Load Distribution	Resistance Distribution	Corrosion	p_f	β
1.35	0.7	Lognormal	Lognormal	No	2.3E-03	2.834
1.35	0.9	Lognormal	Lognormal	No	8.6E-03	2.382
1.35	0.9	Lognormal	Lognormal	Yes	8.7E-03	2.378

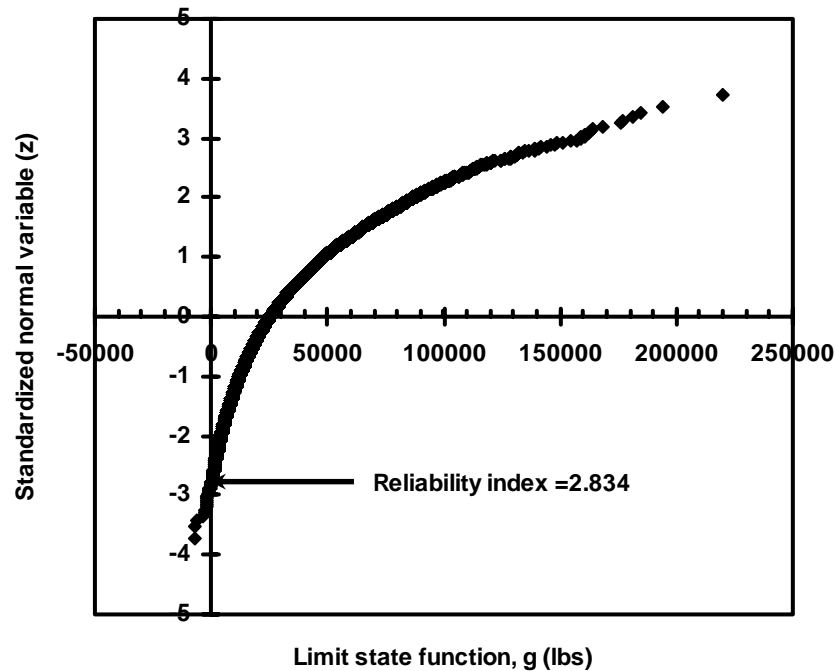


Figure 11. Monte Carlo Analysis Results for Pullout Resistance of Steel Strips Ignoring Corrosion ($\gamma = 1.35$, $\phi = 0.7$)

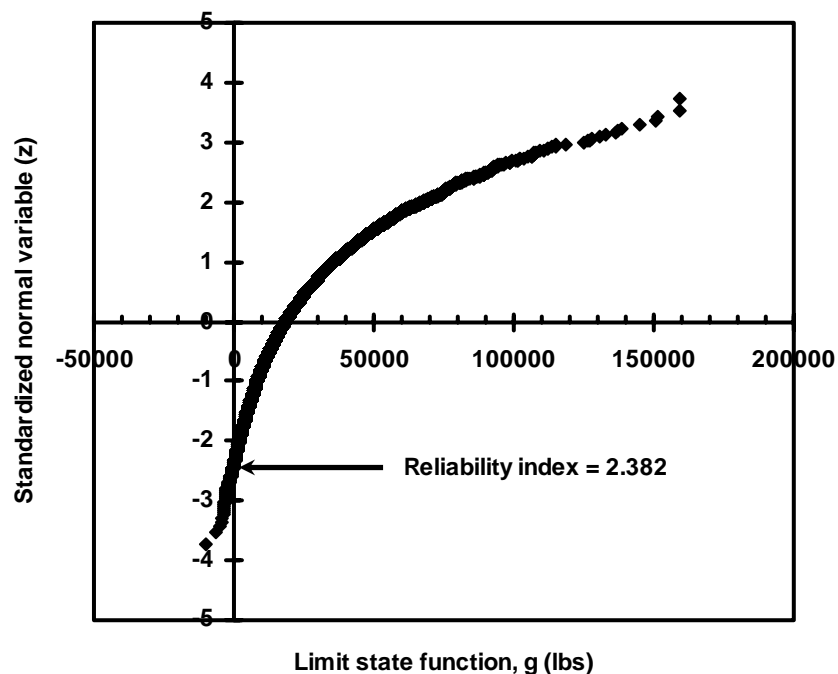


Figure 12. Monte Carlo Analysis Results for Pullout Resistance of Steel Strips Ignoring Corrosion ($\gamma = 1.35$, $\phi = 0.9$)

4.3.2 Calibration of Pullout Resistance for Steel Grids

The pullout resistance of steel grids was calibrated using a lognormal distribution for the load and resistance data based on W test results. Three Monte Carlo simulation analyses were performed and the results are summarized in Table 13. The Monte Carlo simulation input and output reports are presented in Appendix B. For $\phi = 0.7$ at the end of construction (no corrosion), the Monte Carlo simulation resulted in a $p_f = 5.0E-04$ and $\beta = 3.29$ (see Table 13 and Figure 13). For $\phi = 0.9$ at the end of construction (no corrosion), the Monte Carlo simulation resulted in a $p_f = 2.2E-03$ and $\beta = 2.85$ (see Table 13 and Figure 14). For $\phi = 0.9$ at the end of a structure lifetime (considering corrosion), the Monte Carlo simulation resulted in a $p_f = 4.6E-03$ and $\beta = 2.60$ (see Table 13 and Figure 15). Considering the steel corrosion over the design life of the structure (75 years) results in about 9% decrease in the value of β . The resulted β s are within the practical range (3.5 to 2.3) reported for previous LRFD calibrations.

Table 13. Calibration Results of Pullout Resistance for Steel Grids

γ	ϕ	Load Distribution	Resistance Distribution	Corrosion Considered	P_f	β
1.35	0.7	Lognormal	Lognormal	No	5.0E-04	3.29
1.35	0.9	Lognormal	Lognormal	No	2.2E-03	2.85
1.35	0.9	Lognormal	Lognormal	Yes	4.6E-03	2.60

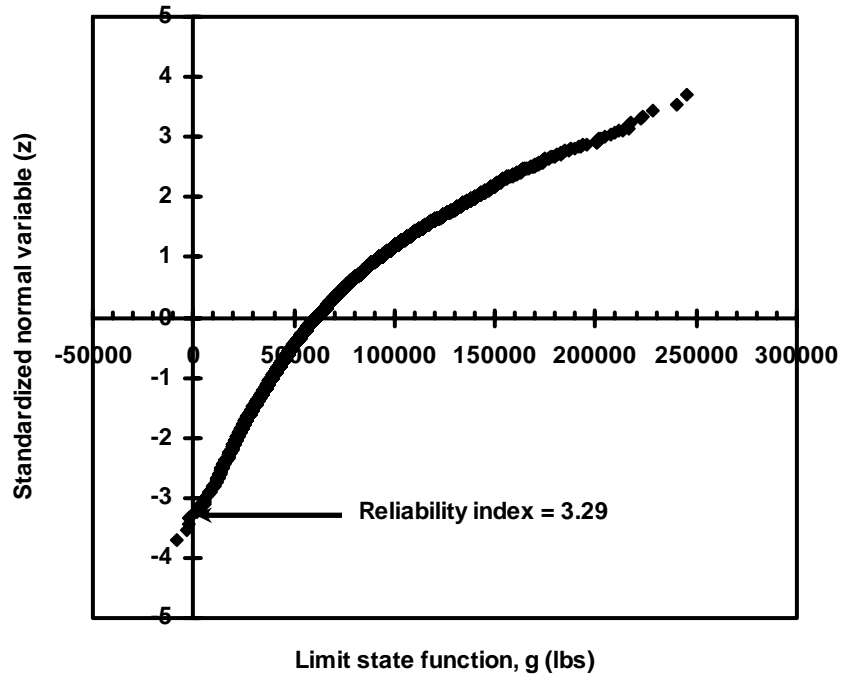


Figure 13. Monte Carlo Analysis Results for Pullout Resistance of Steel Grids Ignoring Corrosion ($\gamma = 1.35$, $\phi = 0.7$)

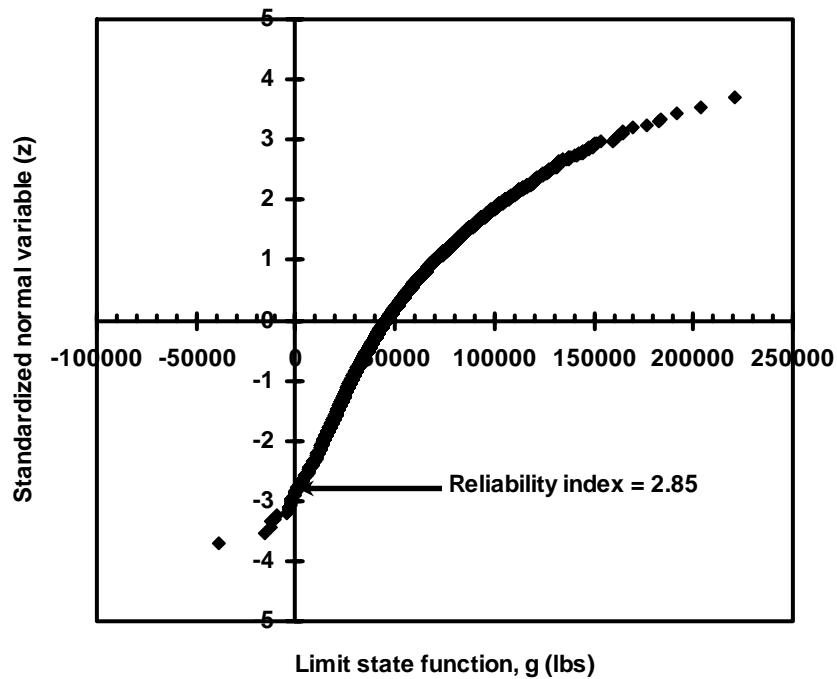


Figure 14. Monte Carlo Analysis Results for Pullout Resistance of Steel Grids Ignoring Corrosion ($\gamma = 1.35$, $\phi = 0.9$)

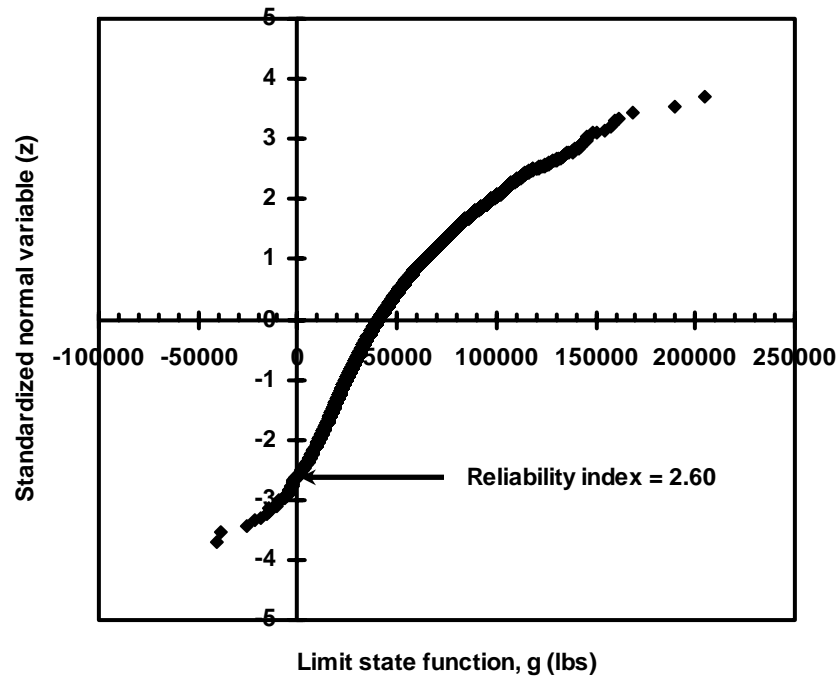


Figure 15. Monte Carlo analysis Results for Pullout Resistance of Steel Grids Considering Corrosion ($\gamma = 1.35$, $\phi = 0.9$)

4.4 Calibration of Rupture Resistance

For calibration of rupture resistance of steel strips, the load factor was fixed at $\gamma = 1.35$, and a value of $\phi = 0.9$ was adopted for the analyses considering the extra rupture capacity in the steel compared to the design loads (see Tables 6 and 7), and the relatively small variability of the bias of the steel yield strength (see Tables 8 and 9). For calibration of the rupture resistance of steel grids, the load factor was fixed at $\gamma = 1.35$, and a value of $\phi = 0.8$ was adopted for the analyses. A lower value of ϕ was adopted for the steel grids to account for the potential of interior wires to be more highly stressed than exterior wires of a grid reinforcement element.

4.4.1 Calibration of Rupture Resistance for Steel Strips

The rupture resistance of steel strips was calibrated using lognormal distributions for the load data based on W test results and normal distribution for the resistance data (Buonopane, et al. 2003). Two Monte Carlo simulation analyses were performed and the results are summarized in Table 14. The Monte Carlo simulation input and output reports are presented in Appendix B. For $\phi = 0.9$ at the end of construction (no corrosion), the Monte Carlo simulation resulted in a $p_f = 1.0E-04$ and $\beta = 3.72$ (see Table 14 and Figure 16). Similar results were obtained using $\phi = 0.9$ and considering corrosion 75 years after construction (see Table 14 and Figure 16). Figure 16 indicates that no rupture failure takes place because g is always above zero. Therefore, the p_f was calculated assuming one g value out of 10,000 could become negative or zero (load exceeds or equal to the resistance).

Table 14. Calibration Results for Rupture Resistance of Steel Strips

γ	ϕ	Load Distribution	Resistance Distribution	Corrosion	P_f	β
1.35	0.9	Lognormal	Normal	No	1.0E-04	3.72
1.35	0.9	Lognormal	Normal	Yes	1.0E-04	3.72

4.4.2 Calibration of Rupture Resistance for Steel Grids

The rupture resistance of steel grids was calibrated using lognormal distribution for the load and based on W test results and normal distribution for the resistance data (Buonopane, et al. 2003).. Two Monte Carlo simulation analyses were performed and the results are summarized in Table 15. The Monte Carlo simulation input and output reports are shown in Appendix B. For $\phi = 0.8$ at the end of construction (no corrosion), the Monte Carlo simulation resulted in a probability of failure of 1.0E-04 and $\beta = 3.72$ (see Table 15 and Figure 17). Similar results were obtained using $\phi = 0.8$ and considering corrosion 75 years after construction (see Table 15 and Figure 17). Figure 17 indicates that no rupture failure may take place because g is always above zero. Therefore, the probability of failure was calculated assuming one g value out of 10,000 could become negative or zero (load exceeds or equal to the resistance).

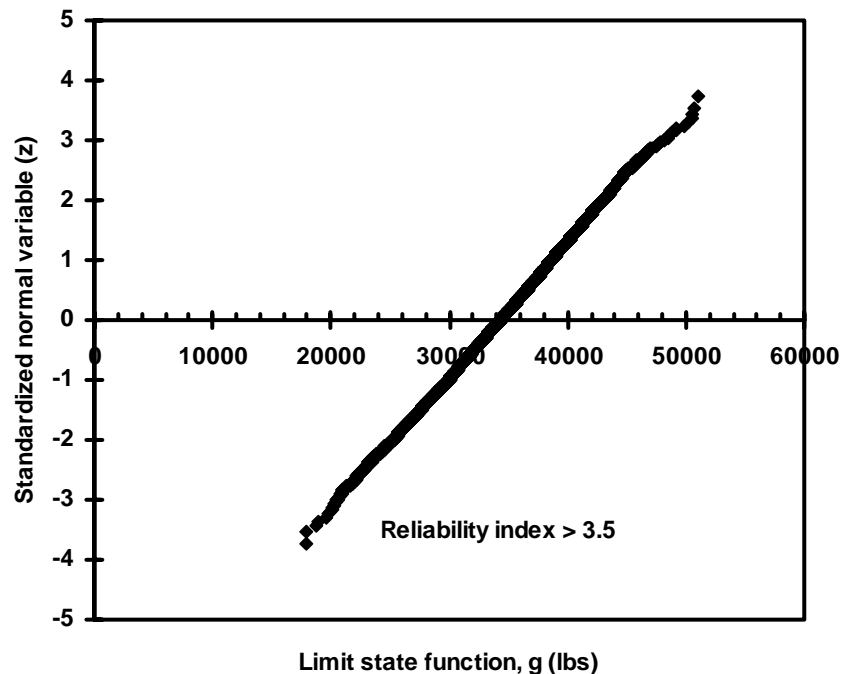


Figure 16. Typical Monte Carlo Analysis Results for Rupture Resistance of Steel Strips ($\gamma = 1.35$, $\phi = 0.9$)

Table 15. Calibration of Rupture Resistance for Steel Grids

γ	ϕ	Load Distribution	Resistance Distribution	Corrosion Considered	Probability of Failure	β
1.35	0.8	Lognormal	Normal	No	1.0E-04	3.72
1.35	0.8	Lognormal	Normal	Yes	1.0E-04	3.72

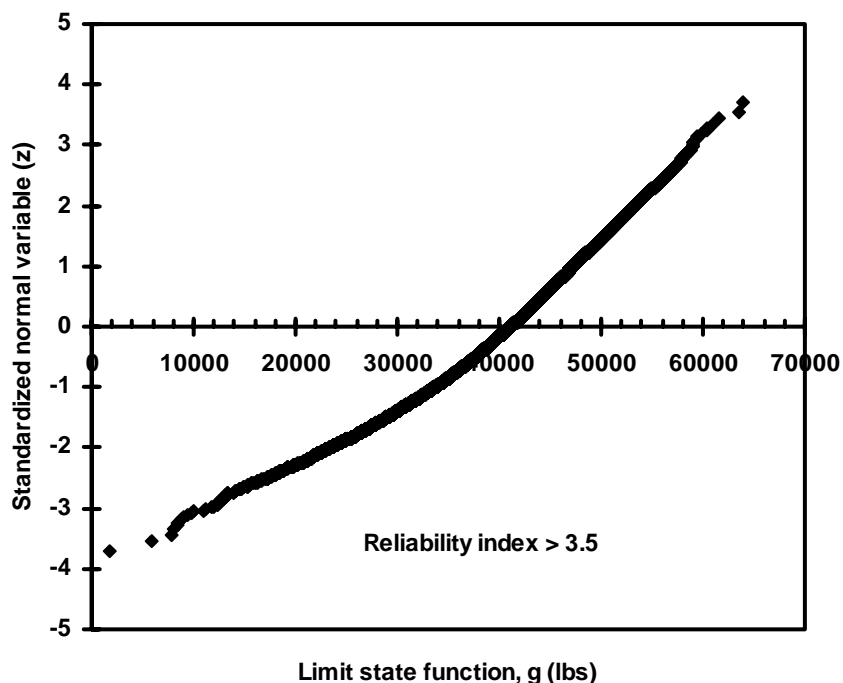


Figure 17. Typical Monte Carlo Analysis Results for Rupture Resistance of Steel Grids ($\gamma = 1.35$, $\phi = 0.8$)

4.5 Verification of Monte Carlo Analysis Results

The reliability indices, β , for pullout and rupture resistance of steel reinforcement can be approximated using closed-form solutions such as shown in Eqs. 8 and 9. Using this approach, the calculated β s from the closed-form solutions can be compared to β s obtained from Monte Carlo analyses. The closed-form solution to calculate β if the load and resistance are both normally distributed is:

$$\beta = \frac{R\lambda_R - Q\lambda_Q}{\sqrt{(\text{COV}_R R\lambda_R)^2 + (\text{COV}_Q Q\lambda_Q)^2}} \quad \text{Eq. 8}$$

If both the load and resistance distributions are lognormally distributed, the closed-form solution to calculate β is:

$$\beta = \frac{\text{LN}\left[\frac{R\lambda_R}{Q\lambda_Q}\right] \sqrt{(1 + \text{COV}_Q^2)/(1 + \text{COV}_R^2)}}{\sqrt{\text{LN}[(1 + \text{COV}_Q^2) * (1 + \text{COV}_R^2)]}} \quad \text{Eq. 9}$$

In these equations, the subletter R refers to the resistance and the subletter Q refers to the load. For example, the resistance-load data for pullout and rupture of steel strips were substituted in Eq. 9 and the results are summarized in Table 16. Calculated β s using Eq. 9 are compared to obtained β s from Monte Carlo analyses (see Table 16).



Table 16. Comparison between β Obtained from Monte Carlo Analysis and β Calculated Using Closed-Form Solution for Steel Strips Without Corrosion

Calibration for:	β From Monte Carlo ($\gamma = 1.35$ and $\phi = 0.9$)	β From Closed-form Solution
Pullout resistance	2.38	2.29
Rupture resistance	>3.5	5.294 (> 3.5)

Table 16 indicates compatibility of β s obtained using the Monte Carlo simulation and β s calculated using a closed form solution.

5. Recommendations

The Monte Carlo calibration analyses resulted in β values consistent with the range for the pullout resistance of steel strips and steel grids from previous LRFD calibrations. The analysis indicated that for $\phi = 0.9$, reasonable β values of 2.38 and 2.60 were computed for pullout resistance of steel strips and steel grids, respectively. The reasonableness of the β values was checked against values determined using closed-form solutions. Based on the results of these analyses, D'Appolonia recommends $\phi = 0.9$ for the pullout resistance of steel strips and steel grids using the Coherent Gravity Method which is the same value prescribed in the *LRFD Specifications* (AASHTO, 2007) for pullout resistance using the Simplified Method.

The calibration analyses of the steel rupture resistance resulted in β values > 3.5, which is greater than typical values of β determined in previous LRFD calibrations. Similar results were obtained using calibration closed-form solutions. The high values of β are attributed to the much higher additional resistance provided by the steel reinforcements at rupture compared to the loads measured in the instrumented test sections which represent service loading. The *LRFD Specifications* (AASHTO, 2007) specify $\phi = 0.75$ for steel strips and $\phi = 0.65$ for steel grids for the Simplified Method, which corresponds to $0.55F_y$ for steel strips and $0.48F_y$ for steel grids in allowable stress design. D'Appolonia believes that the current used ϕ values are overly conservative, and recommends $\phi = 0.90$ for the rupture resistance of steel strips and $\phi = 0.80$ for the rupture resistance of steel grids using the Coherent Gravity Method. A lower ϕ value was adopted for the steel grids to account for the potential of interior wires to be more highly stressed than exterior wires of grid reinforcement.

Acknowledgments

Throughout the course of this project, we received the generous help of several persons in obtaining reference materials needed to complete this study. We therefore acknowledge the assistance of:

- Tony M. Allen, Washington State Department of Transportation
- Professor Loren R. Anderson, Utah State University
- Peter L. Anderson, Reinforced Earth Company
- Dr. Barry R. Christopher, Consultant
- Dr. Kenneth L. Fishman, McMahan and Mann Consulting Engineers, PC
- Professor Patrick J. Fox, The Ohio State University
- Professor Andrzej S. Nowak, University of Nebraska
- Professor Rodrigo Salgado, Purdue University
- Dr. King Sampaco, CH2MHill



References

- Al-Hussaini, M. and E.B. Perry, 1978, "Field Experiment of Reinforced Earth Wall," *Symposium on Earth Reinforcement*, ASCE, New York, NY, pp. 127-156.
- Allen, T.M., B.R. Christopher, V. Elias, and J. DiMaggio, 2001, *Development of the Simplified Method For Internal Stability Design of Mechanically Stabilized Earth Walls*, Washington State Department of Transportation, U.S. Department of Transportation, Federal Highway Administration, 80p.
- Allen, T.M., A.S. Nowak and R.J. Bathurst, 2005, *Calibration to Determine Load and Resistance Factors for Geotechnical and Structural Design*, Transportation Research Circular E-CO79, Transportation Research Board, Washington, DC, 83p.
- AASHTO, 1996, *Standard Specifications for Highway Bridges*, 16th Edition, American Association of State Highway and Transportation Officials, Washington, DC, USA.
- AASHTO, 1999, *Standard Specifications for Highway Bridges*, 16th Edition, 1999 Interim Revisions, American Association of State Highway and Transportation Officials, Washington, DC.
- AASHTO, 2007, *LRFD Bridge Design Specifications*, 4th Edition, American Association of State Highway and Transportation Officials, Washington, DC.
- Anderson, L.R., K.D. Sharp, O.T. Harding, 1987, "Performance of a 50-Foot High Welded Wire Wall," *Soil Improvement – A Ten Year Update*, J.P. Welsh, ed., GSP No. 12, ASCE, pp. 280-308.
- Barker, R.M., J.M. Duncan, K.B. Rojiani, P.S.K. Ooi, C.K. Tan, S.G. and Kim, 1991, *Manuals for the Design of Bridge Foundations: Shallow Foundations, Driven Piles, Retaining Walls and Abutments, Drilled Shafts, Estimating Tolerable Movements, and Load Factor Design Specifications and Commentary*, NCHRP Report 343, TRB, National Research Council, Washington, D.C.
- Bastick, M., 1984, *Reinforced Earth Walls With Short Strips*, Terre Armees Internal Report R-35.
- Bastick, M., F. Schlosser, P. Segrestin, S. Amar and Y. Canepa, 1993, "Experimental Reinforced Earth Structure of Bourron Marlotte: Slender Wall and Abutment Test," *Proceedings, Renforcement Des Sols: Experimentations en Vraie Grandeur des Annees 80*, Paris, 201-228.
- Boyd, M.S., 1993, "Behaviour of a Reinforced Earth Wall at Ngauranga, New Zealand," *Proceedings, Renforcement Des Sols: Experimentations en Vraie Grandeur des Annees 80*, Paris, pp. 229-257.
- Buonopane, S.G., B.W. Schafer, and T. Igusa, 2003, "Reliability Implications of Advanced Analysis in Design of Steel Frames," *Proceedings, ASSCCA '03*, Sydney, Australia.
- Christopher, B.R., 1993, *Deformation Response and Wall Stiffness in Relation to Reinforced Soil Wall Design*, Ph.D. Dissertation, Purdue University, 352p.
- D'Appolonia, 1999, *Developing New AASHTO LRFD Specifications for Retaining Walls*, report prepared for NCHRP 20-7, Task 88, Transportation Research Board, Washington, DC, 63p.
- Elias, V., B.R. Christopher and R.R. Berg, 2001, *Mechanically Stabilized Earth Walls and Reinforced Soil Slopes Design and Construction Guidelines*, National Highway Institute, Federal Highway Administration, U.S. Department of Transportation, Washington, D.C., Report, No. FHWA-NHI-00-043, 394p.
- Hollinghurst, E. and R.T. Murray, 1986, "Reinforced Earth Retaining Wall at A3/A322 Interchange: Design, Construction and Cost," *Proceedings, Institution of Civil Engineers, Part 1*, No. 80, pp. 1327-1341.
- Jakura, K.A., 1988, "Performance of a 62-Foot High Soil Reinforced Wall in California's North Coast Range," California Division of Transportation, Division of New Technology and Research, Office of Transportation Laboratory, Internal Report.
- Lumenaut, 2007, Software, *Manual*, Version 3.4.21, www.lumenaut.com.



- Murray, R.T. and D.M. Farra, D.M., 1990, "Reinforced Earth Wall on the M25 Motorway at Waltham Cross," *Proceedings, Institution of Civil Engineers*, Part 1, No. 88, pp. 261-282.
- Murray, R.T. and E. Hollinghurst, 1986, "Reinforced Earth Retaining Wall at A3/A322 Interchange: Instrumentation, Site Observation and Performance," *Proceedings, Institution of Civil Engineers*, Part 1, No. 80, pp. 1343-1362.
- Neely, W.J., 1993, "Field Performance of a Retained Earth Wall," *Renforcement Des Sols: Experimentations en Vraie Grandeur des Annees 80*, Paris, 171-200.
- Paikowsky, S.G., B. Birgisson, M. McVay, T. Nguyen, C. Kuo, G. Baecher, B. Ayyub, K. Stenersen, K. O'Malley, L. Chernauskas, and M. O'Neill, 2004, *Load and Resistance Factor Design (LRFD) for Deep Foundations*, NCHRP Report 507, Transportation Research Board of the National Academies, Washington, D.C., 126p.
- Richardson, G.N., K.L Lee, A.C. Fong, and D.L. Feger, 1977, "Seismic Testing of Reinforced Earth Walls," *Journal of Geotechnical Engineering Division*, ASCE, Vol. 103, No. GT1, pp. 1-17.
- Runser, D.J., P.J. Fox, and P.L. Bourdeau, 2001, "Field Performance of a 17-m High Reinforced Soil Retaining Wall," *Geosynthetic International*, Vol. 8, No. 5, pp. 367-391.
- Sampaco, C.L., 1995, *Behavior of Welded Wire Mesh Reinforced Soil Walls From Field Evaluation and Finite Element Simulation*, Ph.D. Dissertation, Utah State University, Logan, UT.
- Shapiro, S.S. and M.B. Wilk, 1965, "An Analysis of Variance Test For Normality," *Biometrika* Vol. 52 No. 3, pp. 591-599.
- Singh AK, A. Singh, and M. Engelhardt, 1997, *The Lognormal Distribution in Environmental Applications*, Report EPA/600/R-97/006, U.S. Environmental Protection Agency, Office of Solid Waste and Emergency Response, <http://www.hanford.gov/dqo/training/lognor.pdf>.



Appendix A: Summary of Wall Geometries, Backfill Properties and Steel Reinforcement Details





Table A-1. Summary of Wall Geometry and Backfill Properties

Catalog Number	Wall Height (ft)	Backslope	Backfill Properties			
			Description	Uniformity Coefficient (C _u)	Total Unit Weight (pcf)	Angle of Friction (°)
S1	20.0	Level	Sandy Gravel	7	125	38
S2	12.0	Level	Poorly graded clean concrete sand	2	100	36
S3	19.7	Level	Well graded sand and gravel	40	142	35
S4	19.7	Level	Well graded sand and gravel	40	142	35
S5	20.0	Level	Gravel-sand (46% gravel, 54% sand)	15	130	40
S6	26.2	Level	Well graded sand and gravel	10*	144	34
S7	42.7	Level	Cohesionless soil*	5*	112	36
S8	18.4	Level	Cohesionless soil*	5*	115	44
S9	24.0	Level	Sand	5*	122	37
S10	55.4	Level	Well graded sand with silt	10*	130	38
S11	39.4	Level	Cohesionless Soil	5*	121	38
S12	41.3	5° Negative Slope	Well graded granular greywacke	10	137	35
S13	34.4	Level	Uniformly graded Fontainebleau sand	2	105	36
S14	34.4	Level	Uniformly graded Fontainebleau sand	2	105	36
BM1	20.0	2H:1V Slope	Well graded sandy gravel	43	127	40
BM2	14.1	2H:1V Slope	Well graded sandy gravel	43	127	40
BM3	62.0	1.3° Negative Slope	Gravel with a clayey sand matrix	65	144	32
BM4	20.0	Level	Gravel-sand (46% gravel, 54% sand)	15	130	40
BM5	20.0	Level	Cobbles	2*	105	42
BM6	20.0	Level	Silt	10*	130	35
WW1	50.0	0.5 ft high surcharge	Clean poorly graded sand	2*	120*	30*
WW2	30.0	Level	Poorly graded sand	3	116	38

(*) Based on reported information in the literature and engineering judgment.

Table A-2. Summary of Steel Strip Dimensions, Distribution and Maximum Measured Tension Loads at End of Construction

Catalog number	Vertical spacing, S_v (ft)	Horizontal spacing, S_h (ft)	Strip width, b (in)	Strip thickness, t (in)	$R_c = b/S_h$ (dim)	Depth (ft)	Maximum Measured Tension Load at End of Construction (lbs)
S1	2.50	2.50	3.15	0.12	0.105	1.90	650
	2.50	2.50	3.15	0.12	0.105	6.25	1400
	2.50	2.50	3.15	0.12	0.105	11.25	3650
	2.50	2.50	3.15	0.12	0.105	16.25	4500
	1.25	2.50	3.15	0.12	0.105	19.30	1600
S2*,**	2.00	2.50	4.00	0.03	0.133	3.00	639
	2.00	2.50	4.00	0.03	0.133	7.00	1309
	2.00	2.50	4.00	0.03	0.133	11.00	1176
S3	0.98	2.95	2.95	0.20	0.083	3.90	1326
	0.98	2.95	2.95	0.20	0.083	7.90	1670
	0.98	2.95	2.95	0.20	0.083	9.80	1927
	0.98	2.95	2.95	0.20	0.083	13.80	1799
S4	0.98	2.95	2.95	0.20	0.083	3.90	1713
	0.98	2.95	2.95	0.20	0.083	7.90	1884
	0.98	2.95	2.95	0.20	0.083	9.80	1969
	0.98	2.95	2.95	0.20	0.083	13.80	1713
	0.98	2.95	2.95	0.20	0.083	16.10	2655
S5	2.50	2.40	2.00	0.16	0.069	3.75	2806
	2.50	2.40	2.00	0.16	0.069	8.75	2977
	2.50	2.40	2.00	0.16	0.069	18.75	5755
S6	2.30	2.49	1.57	0.20	0.053	6.89	3109
	2.30	2.49	1.57	0.20	0.053	11.48	2990
	2.30	1.67	1.57	0.20	0.078	16.73	3852
	2.30	1.25	1.57	0.20	0.105	21.33	2153
	2.30	1.02	1.57	0.20	0.129	23.62	3024
S7*	2.46	2.46	3.94	0.13	0.133	6.90	2192
	2.46	2.46	3.94	0.13	0.133	16.90	5676
	2.46	2.46	3.94	0.13	0.133	24.00	9948
	2.46	1.64	3.94	0.13	0.200	31.50	10791
	2.46	1.64	3.94	0.13	0.200	36.00	9948
	2.46	1.64	3.94	0.13	0.200	38.70	9105
	2.46	1.64	3.94	0.13	0.200	41.30	9273
S8*	2.46	1.64	3.15	0.59	0.160	2.46	618
	2.46	1.64	3.15	0.59	0.160	4.92	753
	2.46	1.64	3.15	0.59	0.160	7.38	776
	2.46	1.64	3.15	0.59	0.160	9.84	1079



	2.46	1.64	3.15	0.59	0.160	12.30	809
	2.46	1.64	3.15	0.59	0.160	14.76	1349
	2.46	1.64	3.15	0.59	0.160	17.22	989
S9	2.46	2.46	2.36	0.20	0.080	9.38	2585
	2.46	2.46	2.36	0.20	0.080	11.84	2923
	2.46	2.46	2.36	0.20	0.080	16.77	4272
	2.46	2.46	2.36	0.20	0.080	21.69	6295
S10	2.46	3.28	1.97	0.16	0.050	9.84	5058
	2.46	3.28	1.97	0.16	0.050	19.69	6159
	2.46	3.28	1.97	0.16	0.050	29.53	8790
	2.46	1.64	1.97	0.16	0.100	39.37	7171
S11	2.49	2.49	1.57	0.20	0.053	11.15	3503
	2.49	2.49	1.57	0.20	0.053	21.33	4528
	2.49	2.49	1.57	0.20	0.053	36.09	3451
S12	2.46	2.46	2.36	0.20	0.080	2.46	2091
	2.46	2.46	2.36	0.20	0.080	9.84	3147
	2.46	2.46	2.36	0.20	0.080	19.69	4496
	2.46	1.64	2.36	0.20	0.120	29.53	4047
	2.46	1.64	2.36	0.20	0.120	39.37	5395
S13	2.46	2.46	2.36	0.20	0.080	8.61	3372
	2.46	1.23	2.36	0.20	0.160	15.99	2301
	2.46	1.23	2.36	0.20	0.160	23.38	3069
	2.46	1.23	2.36	0.20	0.160	30.76	3836
S14	2.46	2.46	2.36	0.20	0.080	8.61	3069
	2.46	1.23	2.36	0.20	0.080	15.99	4603
	2.46	1.23	2.36	0.20	0.080	23.38	5513
	2.46	1.23	2.36	0.20	0.160	30.76	3988

(*) Yield strength of steel (F_y) = 51 ksi, however for other wall sections, F_y = 65 ksi

(**) Elastic Young's modulus (E) = 31,100 ksi, however for other wall sections,
E = 29,000 ksi





Table A-3. Summary of Steel Grid Dimensions, Distribution and Maximum Measured Tension Loads at End of Construction

Catalog Number	Steel Bars	Vertical Spacing S_v (ft)	Horizontal Spacing S_h (ft)	Grid Width b (in)	$R_c = b/S_h$	Transverse Steel Spacing S_t (in)	Depth (ft)	Maximum Measured Tension Load at End of Construction (lbs)
BM1	W11 × W11, a mat of 5 longitudinal bars	2.0	3.5	24.0	0.571	24	3.0	899
		2.0	3.5	24.0	0.571	24	7.0	4215
		2.0	3.5	24.0	0.571	24	11.0	3653
		2.0	3.5	24.0	0.571	24	15.0	4496
		2.0	3.5	24.0	0.571	24	19.0	7426
BM2	W11 × W11, a mat of 5 longitudinal bars	2.0	3.5	24.0	0.571	24	3.0	787
		2.0	3.5	24.0	0.571	24	7.0	1753
		2.0	3.5	24.0	0.571	24	11.0	2473
BM3	4W11 × W11	2.5	4.1	17.7	0.363	12	6.3	5876
	6W11 × W11	2.5	4.1	29.5	0.605	24	16.3	7091
	4W20 × W11	2.5	4.1	17.7	0.363	18	26.3	8075
	4W20 × W11	2.5	4.1	17.7	0.363	18	33.7	5411
	6W20 × W11	2.5	4.1	29.5	0.605	24	43.7	16110
	2 (4W20 × W11)	2.5	4.1	41.3	0.847	24	53.7	21481
BM4	W11 × W11, a mat of 4 longitudinal bars	2.5	4.9	18.0	0.284	24	3.8	2893
		2.5	4.9	18.0	0.284	24	8.8	14467
		2.5	4.9	18.0	0.284	24	16.3	9063
		2.5	4.9	18.0	0.284	24	18.8	3480
BM5	W11 × W11, a mat of 4 longitudinal bars	2.5	4.9	18.0	0.284	24	3.8	1313
		2.5	4.9	18.0	0.284	24	8.8	1517
		2.5	4.9	18.0	0.284	24	16.3	12390



Catalog Number	Steel Bars	Vertical Spacing S_v (ft)	Horizontal Spacing S_h (ft)	Grid Width b (in)	$R_c = b/S_h$	Transverse Steel Spacing S_t (in)	Depth (ft)	Maximum Measured Tension Load at End of Construction (lbs)
BM6	W11 × W11, a mat of 4 longitudinal bars	2.5	4.9	18.0	0.284	24	3.8	535
		2.5	4.9	18.0	0.284	24	6.3	14862
		2.5	4.9	18.0	0.284	24	13.8	11357
		2.5	4.9	18.0	0.284	24	16.3	8489
WW1	W4.5 × W3.5	1.5	0.5	6.0	1.000	9	10.3	503
	W7 × W3.5	1.5	0.5	6.0	1.000	9	19.1	815
	W7 × W3.5	1.5	0.5	6.0	1.000	9	26.5	936
	W9.5 × W3.5	1.5	0.5	6.0	1.000	9	33.8	1241
	W9.5 × W3.5	1.5	0.5	6.0	1.000	9	41.2	1374
	W12 × W5	1.5	0.5	6.0	1.000	9	45.6	1271
	W12 × W5	1.5	0.5	6.0	1.000	9	50.0	1025
WW2	W4.5 × W7, 9 longitudinal bars	2.5	6.7	48.0	0.595	24	1.5	900
	W4.5 × W7, 9 longitudinal bars	2.5	6.7	48.0	0.595	24	4.0	2732
	W9.5 × W7, 9 longitudinal bars	2.5	6.7	48.0	0.595	24	9.0	6912
	W12 × W7, 9 longitudinal bars	2.5	6.7	48.0	0.595	24	14.0	12056



Catalog Number	Steel Bars	Vertical Spacing S_v (ft)	Horizontal Spacing S_h (ft)	Grid Width b (in)	$R_c = b/S_h$	Transverse Steel Spacing S_t (in)	Depth (ft)	Maximum Measured Tension Load at End of Construction (lbs)
	W12 × W7, 9 longitudinal bars	2.5	6.7	48.0	0.595	24	17.0	5787
	W14 × W7, 9 longitudinal bars	2.5	6.7	48.0	0.595	24	21.5	10769
		2.5	6.7	48.0	0.595	24	27.0	7232
		2.5	6.7	48.0	0.595	24	29.0	3695

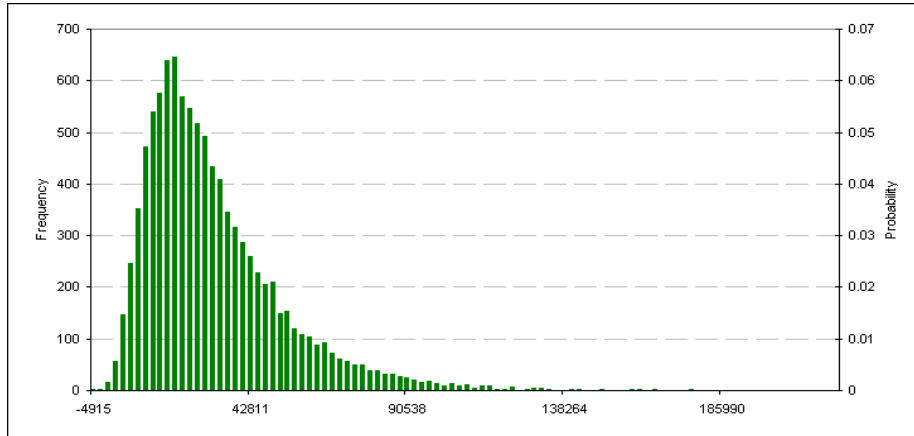
Appendix B: Calibration Results of Steel Pullout Resistance and Steel Rupture Resistance Using Monte Carlo Analysis



Monte Carlo Analysis Report For Pullout Resistance of Steel Strips Ignoring Corrosion, $\gamma = 1.35$ and $\phi = 0.7$

Lumenaut Simulation Report

Output Cell: MC Input!\$B\$26 Workbook: P-S-L-0.7.xls
 Output Name: g Date: 10-Oct-07
 Iterations: 10000 Time: 12:39:58 PM



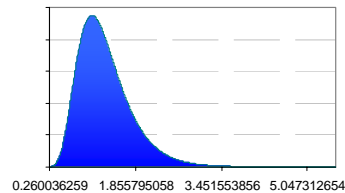
Percentile	Min to Max
0%	-7187.498113
10%	9591.312291
20%	13887.13401
30%	17639.39079
40%	21336.63497
50%	25413.44842
60%	30006.74894
70%	35973.4175
80%	44137.16527
90%	57836.59976
100%	220079.8156

Percentile	Max to Min
0%	220079.8156
10%	57836.59976
20%	44137.16527
30%	35973.4175
40%	30006.74894
50%	25413.44842
60%	21336.63497
70%	17639.39079
80%	13887.13401
90%	9591.312291
100%	-7187.498113

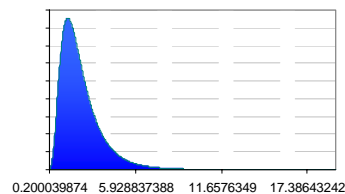
Mean	30491.63706
Median	25413.15677
Mode	1.79055E+22
Stand. Deviation	21358.16078
Variance	456171031.9
Mean Std. Error	213.5816078
Range	227267.3137
Range Min	-7187.498113
Range Max	220079.8156
Skewness	1.800785887
Kurtosis	5.605480542

Lumenaut Simulation Input

Cell Name: Load bias
 Cell: MC Input!\$B\$17
 Distribution: Lognormal
 Mean: 1.294
 Stand. Dev.: 0.5
 Min: 0.260036259
 Max: 5.579232253



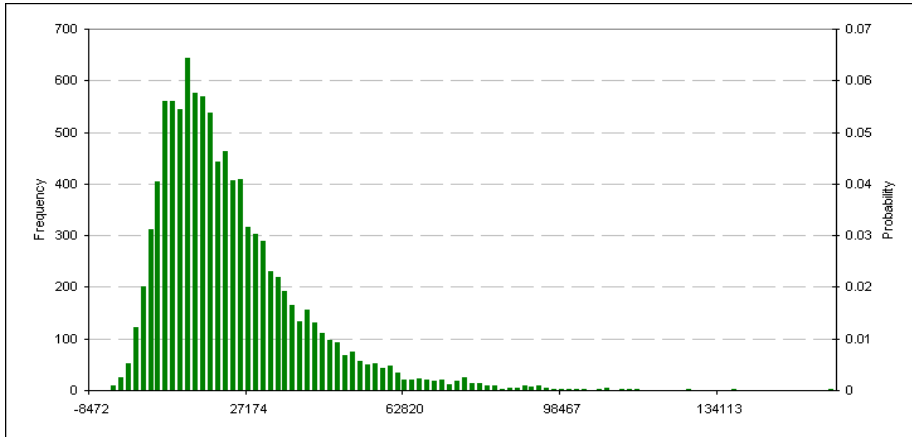
Cell Name: Pullout bias
 Cell: MC Input!\$B\$7
 Distribution: Lognormal
 Mean: 2.28
 Stand. Dev.: 1.38
 Min: 0.200039874
 Max: 19.29603159



Monte Carlo Analysis Report For Pullout Resistance of Steel Strips Ignoring Corrosion, $\gamma = 1.35$ and $\phi = 0.9$

Lumenaut Simulation Report

Output Cell:	MC Input!\$B\$26	Workbook:	P-S-L-0.9.xls
Output Name:	g	Date:	10-Oct-07
Iterations:	10000	Time:	12:44:46 PM



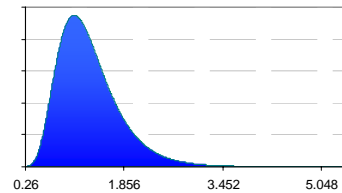
Percentile	Min to Max
0%	-10169.93672
10%	6307.598857
20%	9505.705468
30%	12463.60493
40%	15250.27643
50%	18329.88846
60%	22010.15987
70%	26319.36423
80%	32473.41312
90%	42927.68951
100%	159574.8736

Percentile	Max to Min
0%	159574.8736
10%	42927.68951
20%	32473.41312
30%	26319.36423
40%	22010.15987
50%	18329.88846
60%	15250.27643
70%	12463.60493
80%	9505.705468
90%	6307.598857
100%	-10169.93672

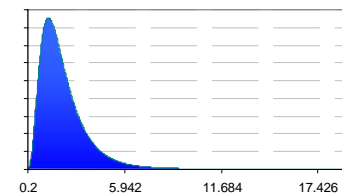
Mean	22294.70967
Median	18329.62234
Mode	7.23533E+21
Stand. Deviation	16647.81775
Variance	277149835.8
Mean Std. Error	166.4781775
Range	169744.8103
Range Min	-10169.93672
Range Max	159574.8736
Skewness	1.912667027
Kurtosis	6.420463075

Lumenaut Simulation Input

Cell Name:	Load bias
Cell:	MC Input!\$B\$17
Distribution:	Lognormal
Mean:	1.294
Stand. Dev.:	0.5
Min:	0.26
Max:	5.58



Cell Name:	Pullout bias
Cell:	MC Input!\$B\$7
Distribution:	Lognormal
Mean:	2.28
Stand. Dev.:	1.38
Min:	0.2
Max:	19.34

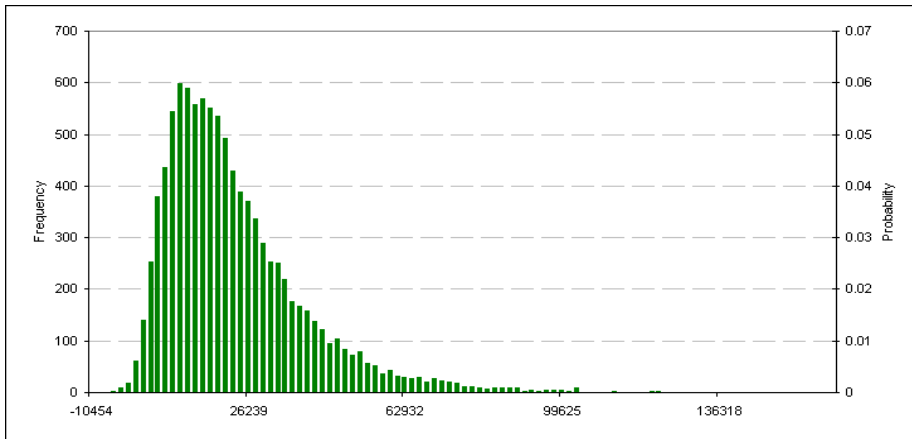


Monte Carlo Analysis Report For Pullout Resistance of Steel Strips Considering Corrosion, $\gamma = 1.35$ and $\phi = 0.9$



Lumenaut Simulation Report

Output Cell: MC Input!\$B\$26 **Workbook:** P-S-L-0.9-corrosion.xls
Output Name: g **Date:** 11-Oct-07
Iterations: 10000 **Time:** 1:42:52 PM



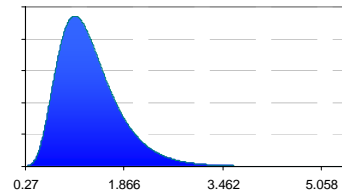
Percentile	Min to Max
0%	-12200.86329
10%	5864.948739
20%	9308.47782
30%	12154.56238
40%	15264.68972
50%	18379.38731
60%	22071.82001
70%	26614.55641
80%	32801.09411
90%	43246.27833
100%	162527.6084

Percentile	Max to Min
0%	162527.6084
10%	43246.27833
20%	32801.09411
30%	26614.55641
40%	22071.82001
50%	18379.38731
60%	15264.68972
70%	12154.56238
80%	9308.47782
90%	5864.948739
100%	-12200.86329

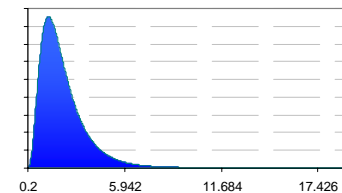
Mean	22197.9601
Median	18377.66283
Mode	5.50244E+21
Stand. Deviation	16418.7504
Variance	269575364.7
Mean Std. Error	164.187504
Range	174728.4717
Range Min	-12200.86329
Range Max	162527.6084
Skewness	1.664016357
Kurtosis	4.572478427

Lumenaut Simulation Input

Cell Name: Load bias
Cell: MC Input!\$B\$17
Distribution: Lognormal
Mean: 1.314
Stand. Dev.: 0.502
Min: 0.27
Max: 5.59



Cell Name: Pullout bias
Cell: MC Input!\$B\$7
Distribution: Lognormal
Mean: 2.28
Stand. Dev.: 1.38
Min: 0.2
Max: 19.34

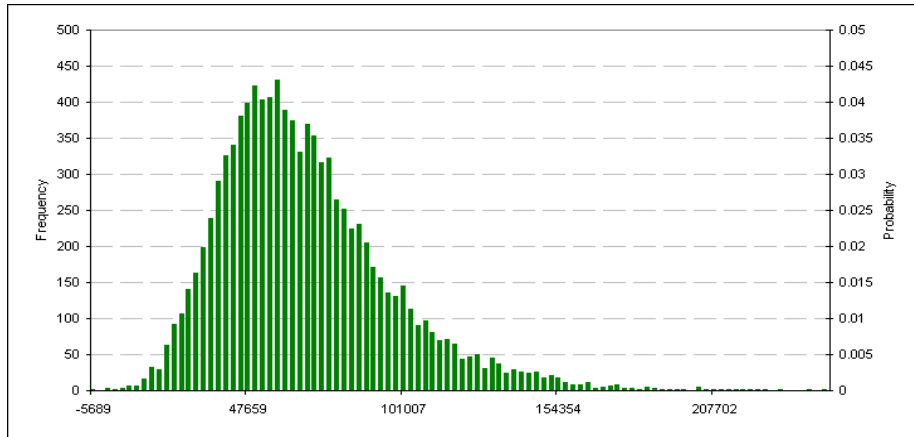


Monte Carlo Analysis Report For Pullout Resistance of Steel Grids Ignoring Corrosion, $\gamma = 1.35$ and $\phi = 0.7$



Lumenaut Simulation Report

Output Cell: MC Input!\$C\$26 Workbook: P-G-L-0.7.xls
 Output Name: g Date: 10-Oct-07
 Iterations: 10000 Time: 2:31:15 PM



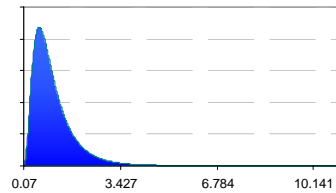
Percentile	Min to Max
0%	-8229.045129
10%	33963.30023
20%	42168.76109
30%	48682.66773
40%	54775.30568
50%	61162.59978
60%	68255.78646
70%	76032.57453
80%	86654.93261
90%	103837.3435
100%	245807.0433

Percentile	Max to Min
0%	245807.0433
10%	103837.3435
20%	86654.93261
30%	76032.57453
40%	68255.78646
50%	61162.59978
60%	54775.30568
70%	48682.66773
80%	42168.76109
90%	33963.30023
100%	-8229.045129

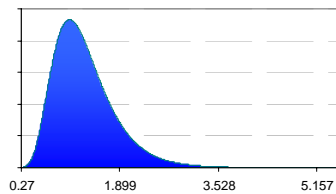
Mean	65941.735
Median	61161.48023
Mode	3.71923E+22
Stand. Deviation	29272.46501
Variance	856877208
Mean Std. Error	292.7246501
Range	254036.0884
Range Min	-8229.045129
Range Max	245807.0433
Skewness	1.094687306
Kurtosis	2.065936455

Lumenaut Simulation Input

Cell Name: Load bias
 Cell: MC Input!\$C\$17
 Distribution: Lognormal
 Mean: 1.084
 Stand. Dev.: 0.737
 Min: 0.07
 Max: 11.26



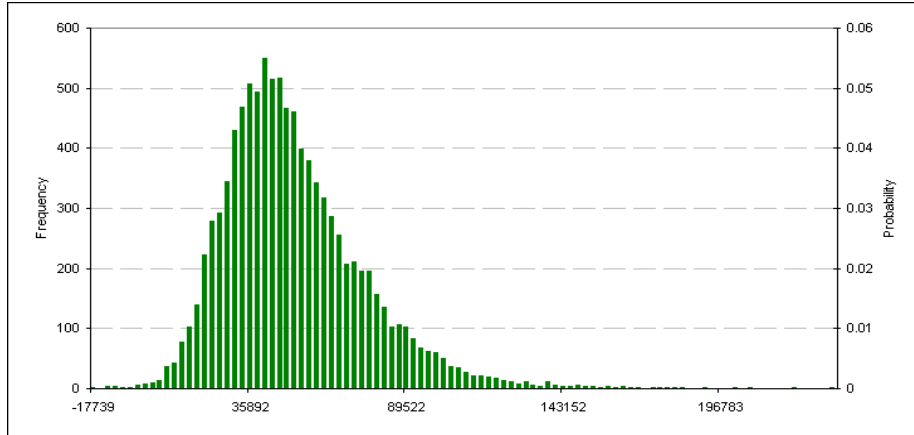
Cell Name: Resistance bias
 Cell: MC Input!\$C\$7
 Distribution: Lognormal
 Mean: 1.318049404
 Stand. Dev.: 0.51
 Min: 0.27
 Max: 5.7



Monte Carlo Analysis Report For Pullout Resistance of Steel Grids Ignoring Corrosion, $\gamma = 1.35$ and $\phi = 0.9$

Lumenaut Simulation Report

Output Cell:	MC Input!\$C\$26	Workbook:	P-G-L-0.9.xls
Output Name:	g	Date:	10-Oct-07
Iterations:	10000	Time:	2:36:01 PM



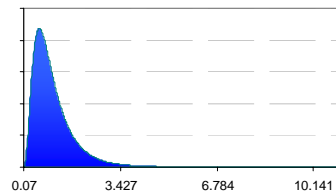
Percentile	Min to Max
0%	-20292.62819
10%	23548.26621
20%	30690.42661
30%	35940.54789
40%	40875.1297
50%	45716.25398
60%	51257.51522
70%	58075.57777
80%	66797.17102
90%	80448.78167
100%	235090.0705

Percentile	Max to Min
0%	235090.0705
10%	80448.78167
20%	66797.17102
30%	58075.57777
40%	51257.51522
50%	45716.25398
60%	40875.1297
70%	35940.54789
80%	30690.42661
90%	23548.26621
100%	-20292.62819

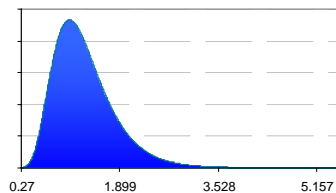
Mean	49680.42107
Median	45715.05252
Mode	1.79006E+22
Stand. Deviation	23652.56178
Variance	559443678.7
Mean Std. Error	236.5256178
Range	255382.6987
Range Min	-20292.62819
Range Max	235090.0705
Skewness	1.120796226
Kurtosis	2.720039537

Lumenaut Simulation Input

Cell Name:	Load bias
Cell:	MC Input!\$C\$17
Distribution:	Lognormal
Mean:	1.084
Stand. Dev.:	0.737
Min:	0.07
Max:	11.26



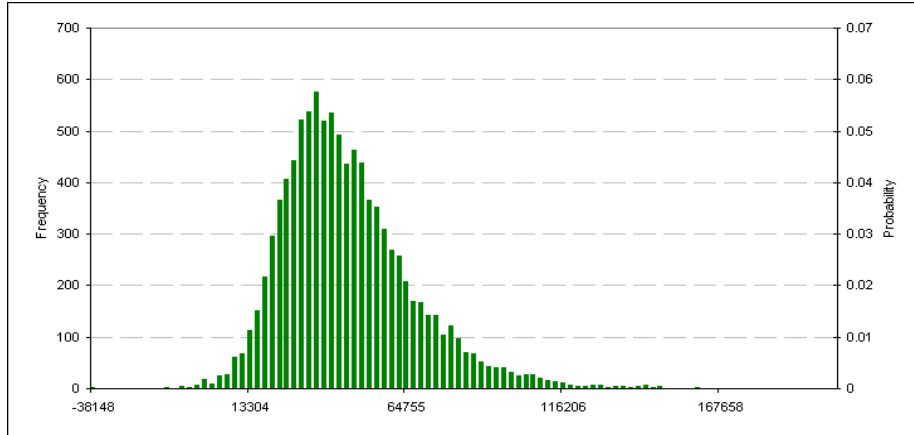
Cell Name:	Resistance bias
Cell:	MC Input!\$C\$7
Distribution:	Lognormal
Mean:	1.318049404
Stand. Dev.:	0.51
Min:	0.27
Max:	5.7



Monte Carlo Analysis Report For Pullout Resistance of Steel Grids Considering Corrosion, $\gamma = 1.35$ and $\phi = 0.9$

Lumenaut Simulation Report

Output Cell: MC Input!\$C\$26 **Workbook:** P-G-L-0.9-corrosion.xls
Output Name: g **Date:** 10-Oct-07
Iterations: 10000 **Time:** 2:50:22 PM



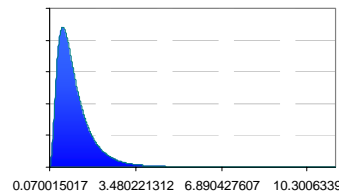
Percentile	Min to Max
0%	-40597.96995
10%	20617.87966
20%	26695.69343
30%	31731.16218
40%	36062.06698
50%	40708.39302
60%	45960.02065
70%	51766.26122
80%	59466.83879
90%	72677.19551
100%	204408.6173

Percentile	Max to Min
0%	204408.6173
10%	72677.19551
20%	59466.83879
30%	51766.26122
40%	45960.02065
50%	40708.39302
60%	36062.06698
70%	31731.16218
80%	26695.69343
90%	20617.87966
100%	-40597.96995

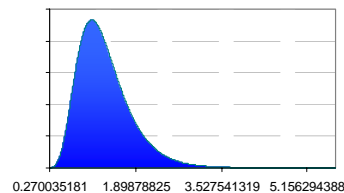
Mean	44126.37009
Median	40707.03241
Mode	1.18838E+22
Stand. Deviation	21653.03827
Variance	468854066.4
Mean Std. Error	216.5303827
Range	245006.5872
Range Min	-40597.96995
Range Max	204408.6173
Skewness	1.05733772
Kurtosis	2.406611895

Lumenaut Simulation Input

Cell Name: Load bias
Cell: MC Input!\$C\$17
Distribution: Lognormal
Mean: 1.069
Stand. Dev.: 0.74
Min: 0.070015017
Max: 11.43736933



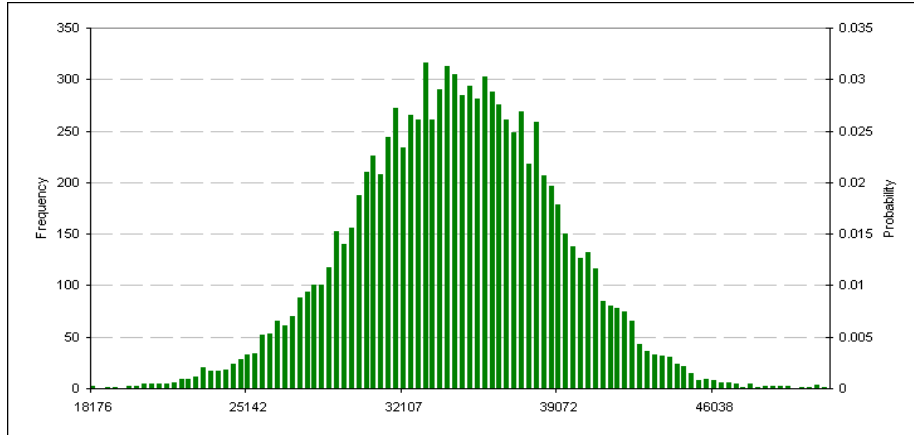
Cell Name: Resistance bias
Cell: MC Input!\$C\$7
Distribution: Lognormal
Mean: 1.318049404
Stand. Dev.: 0.51
Min: 0.270035181
Max: 5.699212077



Monte Carlo Analysis Report For Rupture Resistance of Steel Strips Ignoring Corrosion, $\gamma = 1.35$ and $\phi = 0.9$

Lumenaut Simulation Report

Output Cell:	MC Input!\$D\$26	Workbook:	R-S-L-N-0.9.xls
Output Name:	g	Date:	11-Oct-07
Iterations:	10000	Time:	1:30:54 PM



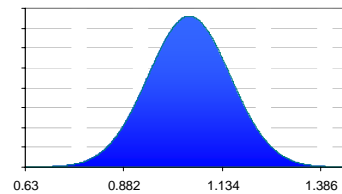
Percentile	Min to Max
0%	17844.54509
10%	28611.79988
20%	30577.51987
30%	31987.61666
40%	33195.51516
50%	34320.51223
60%	35476.30193
70%	36644.31794
80%	37969.03171
90%	39879.80886
100%	51012.7151

Percentile	Max to Min
0%	51012.7151
10%	39879.80886
20%	37969.03171
30%	36644.31794
40%	35476.30193
50%	34320.51223
60%	33195.51516
70%	31987.61666
80%	30577.51987
90%	28611.79988
100%	17844.54509

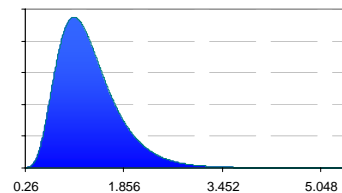
Mean	34275.61205
Median	34320.43265
Mode	1.1851E+19
Stand. Deviation	4424.560331
Variance	19576734.12
Mean Std. Error	44.24560331
Range	33168.17001
Range Min	17844.54509
Range Max	51012.7151
Skewness	-0.067608842
Kurtosis	0.092560291

Lumenaut Simulation Input

Cell Name:	Resistance bias
Cell:	MC Input!\$B\$12
Distribution:	Normal
Mean:	1.05
Standard Deviantio	0.105
Min:	0.6302
Max:	1.4698



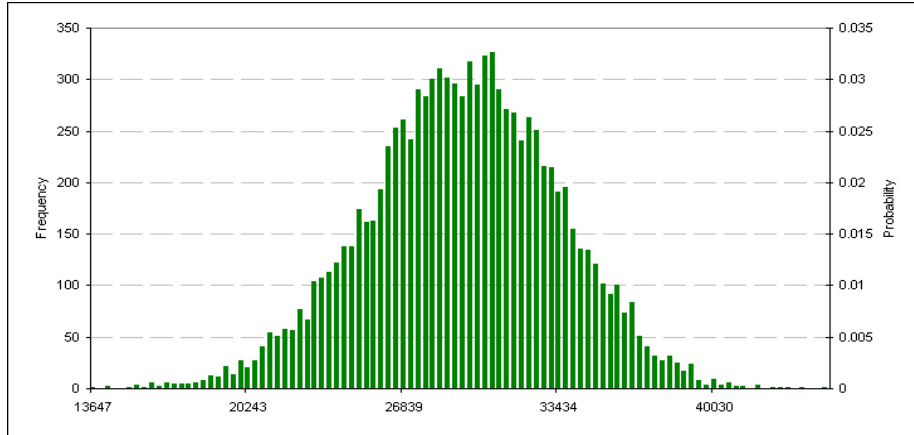
Cell Name:	Load bias
Cell:	MC Input!\$B\$17
Distribution:	Lognormal
Mean:	1.294
Stand. Dev.	0.5
Min:	0.26
Max:	5.58



Monte Carlo Analysis Report For Rupture Resistance of Steel Strips Considering Corrosion, $\gamma = 1.35$ and $\phi = 0.9$

Lumenaut Simulation Report

Output Cell:	MC Input!\$D\$26	Workbook:	R-S-L-N-0.9-corrosion.xls
Output Name:	g	Date:	11-Oct-07
Iterations:	10000	Time:	1:32:36 PM



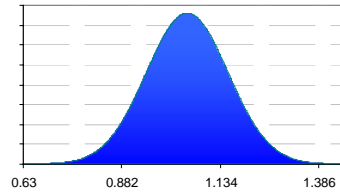
Percentile	Min to Max
0%	13333.06209
10%	23939.31513
20%	25894.96488
30%	27166.18183
40%	28230.80192
50%	29288.4998
60%	30298.68466
70%	31377.49824
80%	32635.99972
90%	34358.5903
100%	44741.47152

Percentile	Max to Min
0%	44741.47152
10%	34358.5903
20%	32635.99972
30%	31377.49824
40%	30298.68466
50%	29288.4998
60%	28230.80192
70%	27166.18183
80%	25894.96488
90%	23939.31513
100%	13333.06209

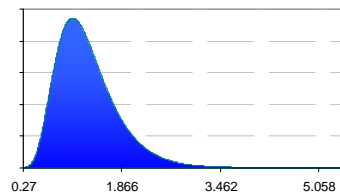
Mean	29205.23591
Median	29288.4251
Mode	8.10589E+18
Stand. Deviation	4049.442829
Variance	16397987.22
Mean Std. Error	40.49442829
Range	31408.40943
Range Min	13333.06209
Range Max	44741.47152
Skewness	-0.121894724
Kurtosis	0.014830994

Lumenaut Simulation Input

Cell Name:	Resistance bias
Cell:	MC Input!\$B\$12
Distribution:	Normal
Mean:	1.05
Standard Deviantio	0.105
Min:	0.6302
Max:	1.4698



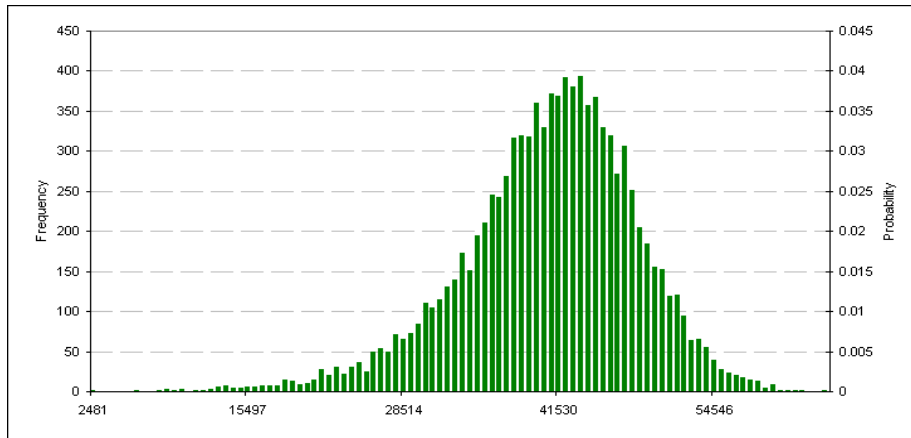
Cell Name:	Load bias
Cell:	MC Input!\$B\$17
Distribution:	Lognormal
Mean:	1.314
Stand. Dev.	0.502
Min:	0.27
Max:	5.59



Monte Carlo Analysis Report For Rupture Resistance of Steel Grids Ignoring Corrosion, $\gamma = 1.35$ and $\phi = 0.8$

Lumenaut Simulation Report

Output Cell: MC Input!\$E\$26 Workbook: R-G-L-N-0.8.xls
 Output Name: g Date: 10-Oct-07
 Iterations: 10000 Time: 3:41:38 PM



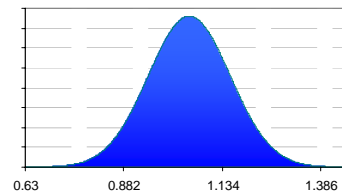
Percentile	Min to Max
0%	1861.41014
10%	31073.94559
20%	35051.80787
30%	37495.48542
40%	39374.92213
50%	41134.37419
60%	42746.94362
70%	44414.83702
80%	46387.09772
90%	48977.32313
100%	63843.42767

Percentile	Max to Min
0%	63843.42767
10%	48977.32313
20%	46387.09772
30%	44414.83702
40%	42746.94362
50%	41134.37419
60%	39374.92213
70%	37495.48542
80%	35051.80787
90%	31073.94559
100%	1861.41014

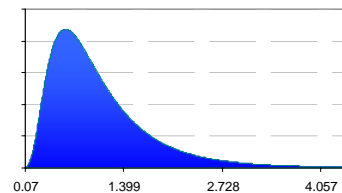
Mean	40460.98333
Median	41134.28666
Mode	1.11889E+20
Stand. Deviation	7267.289643
Variance	52813498.75
Mean Std. Error	72.67289643
Range	61982.01753
Range Min	1861.41014
Range Max	63843.42767
Skewness	-0.618245141
Kurtosis	1.011828845

Lumenaut Simulation Input

Cell Name: Resistance
 Cell: MC Input!\$B\$12
 Distribution: Normal
 Mean: 1.05
 Standard Deviantio: 0.105
 Min: 0.6301
 Max: 1.4699



Cell Name: Load
 Cell: MC Input!\$C\$17
 Distribution: Lognormal
 Mean: 1.084
 Stand. Dev.: 0.737
 Min: 0.07
 Max: 4.5

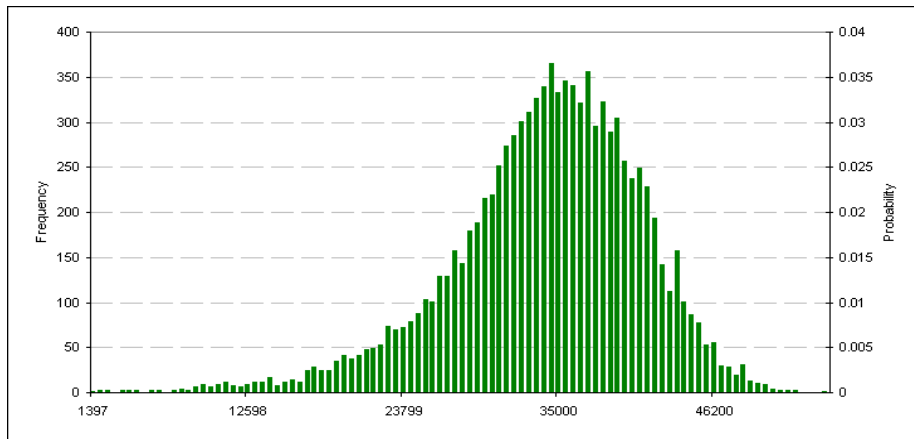


Monte Carlo Analysis Report For Rupture Resistance of Steel Grids Considering Corrosion, $\gamma = 1.35$ and $\phi = 0.8$



Lumenaut Simulation Report

Output Cell: MC Input!\$E\$26 **Workbook:** R-G-L-N-0.8-Corrosion.xls
Output Name: g **Date:** 10-Oct-07
Iterations: 10000 **Time:** 3:39:33 PM



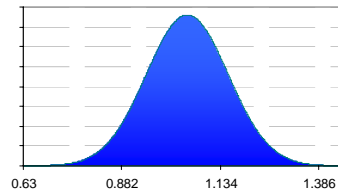
Percentile	Min to Max
0%	863.8260372
10%	25075.9793
20%	28834.15978
30%	31174.63325
40%	32930.29425
50%	34505.55098
60%	36058.16695
70%	37711.12177
80%	39482.28259
90%	41747.86369
100%	54200.89192

Percentile	Max to Min
0%	54200.89192
10%	41747.86369
20%	39482.28259
30%	37711.12177
40%	36058.16695
50%	34505.55098
60%	32930.29425
70%	31174.63325
80%	28834.15978
90%	25075.9793
100%	863.8260372

Mean	33850.86899
Median	34502.60241
Mode	9.26979E+19
Stand. Deviation	6860.167619
Variance	47061899.76
Mean Std. Error	68.60167619
Range	53337.06588
Range Min	863.8260372
Range Max	54200.89192
Skewness	-0.751413912
Kurtosis	1.185761156

Lumenaut Simulation Input

Cell Name: Resistance
Cell: MC Input!\$B\$12
Distribution: Normal
Mean: 1.05
Standard Deviantio: 0.105
Min: 0.6301
Max: 1.4699



Cell Name: Load
Cell: MC Input!\$C\$17
Distribution: Lognormal
Mean: 1.069
Stand. Dev. 0.74
Min: 0.07
Max: 4.5

